International Journal of Solids and Structures xxx (2015) xxx–xxx

Contents lists available at ScienceDirect

International Journal of Solids and Structures

journal homepage: www.elsevier.com/locate/ijsolstr

Graphene resting on substrate: Closed form solutions for the perfect bonding and the delamination case

D. Sfyris [a,*], Ch. Androulidakis [a], C. Galiotis [a,b]

[a] Foundation for Research and Technology, Institute of Chemical Engineering, Stadiou Strees, Platani, Patras GR-26504, Greece
[b] University of Patras, Department of Chemical Engineering, Greece

ARTICLE INFO

Article history:
Received 13 February 2015
Received in revised form 4 May 2015
Available online xxxx

Keywords:
Graphene
Hexagonal 2-lattice
Substrate
Perfect bonding
Delamination

ABSTRACT

We study closed form solutions for the perfect bonding and the delamination case for a monolayer graphene sheet resting on an elastic foundation. The theoretical framework we adopt is restricted to the materially and geometrically linear case. Graphene is modeled as a hexagonal 2-lattice, while the substrate is assumed to behave in an isotropic linearly elastic manner. Initially, we ignore out-of-surface motions and study the case of biaxial tension/compression and simple shear. We find the components of the shift vector by solving the equations ruling the shift vector. We then substitute this expression for the shift vector components to the momentum equation. This way we obtain conditions that the field of the internal strains, the strain constants and the material parameters should satisfy in order biaxial tension/compression and simple shear to be solutions for all equilibrium equations. For the particular case of axial strain and for the simple shear case we plot the mean stress components versus strain for three different substrates. Then, we take into account out-of-surface motions. We assume the out-of-surface displacement to be the product of a wave-like function and an unknown function, which we determine under certain conditions. These conditions are constraints that the field of the internal strains, the strain constant and the material characteristics of the substrate and graphene should satisfy in order the equilibrium equations to be satisfied. These cases pertain to the perfect bonding case. Distinguishing film's displacement from the bulk (substrate) displacement we study the case where delamination occur. We again use a semi-inverse method: we assume film's displacement to be the product of a wave-like function with an unknown function. The bulk's displacement is assumed to be different from the one of the film, in areas of delamination. We determine the unknown function present in the displacement of the film, by requiring the momentum equations to be satisfied.

1. Introduction

Graphene is a two-dimensional sheet that constitutes the building unit of all graphitic forms of matter, such as graphite, carbon nanotubes and carbon fibers. Graphene attract much attention to the mechanics community due to its very high strength of approximately 1 TPa (Lee et al., 2008). This together with its very small thickness, of approximately 0.335 nm, makes graphene an ideal potential candidate for strengthening composite structures. In a recent article we review the mechanical properties of graphene as probed by spectroscopic measurements and as calculated by ab initio, molecular simulation and continuum mechanical methods (Galiotis et al., in press).

On the other hand, graphene's very small thickness has some unpleasant consequences when trying to subject it to experiments: it is very difficult to grab graphene and apply some kind of loading. To remedy this situation workers embed graphene samples on a polymer substrate and load the system graphene/substrate. Then the technique of Raman spectroscopy can be applied to measure the mechanical properties of graphene by measuring the G and 2D peak of the Raman spectra. In Androulidakis et al. (2014) we embed a graphene flake on a substrate and apply a tensional loading to the system graphene/substrate using either the technique of cantilever beam or the four point bending technique.

The present work is motivated from the above described use of the substrate. It targets to mathematically model the graphene/-substrate system when subjected to simple loadings. In a sense, this is a continuation of our previous efforts to model free-standing graphene (Sfyris and Galiotis, in press; Sfyris et al., 2014a,b; Sfyris et al., in press), by taking into account substrate's

* Corresponding author. Tel./fax: +30 2610 965 272.
E-mail addresses: dsfyris@iceht.forth.gr, dsfyris@sfyris.net (D. Sfyris).
URL: http://www.sfyris.net (D. Sfyris).

http://dx.doi.org/10.1016/j.ijsolstr.2015.06.024
0020-7683/

presence. In Sfyris and Galiotis (in press), Sfyris et al. (2014a,b) and Sfyris et al. (in press) we present the mathematical background for modeling graphene at the continuum level. In particular, adopting the framework of Steigmann and Ogden (1999) we utilize a surface free energy for graphene based on three arguments. The first argument is an in-surface stain measure describing changes taking place on the surface. The second argument is the curvature tensor which describe the out-of-surface motion and introduce bending into the model. The third argument is the shift vector. The motivation for assuming the shift vector as an argument stem from well established theories of crystalline materials (Parry, 1978; Ericksen, 1970; Ericksen, 1979; Fadda and Zanzotto, 2000; Fadda and Zanzotto, 2001; Pitteri, 1984; Pitteri, 1985; Pitteri and Zanzotto, 2003).

In this sense we stress that graphene is modeled as a hexagonal 2-lattice (Sfyris and Galiotis, in press; Sfyris et al., 2014a,b).The need for viewing graphene as a multilattice stem from the fact that graphene's lattice cannot be seen as a Bravais simple lattice. In standard terminology of applied crystallography (Fadda and Zanzotto, 2000; Fadda and Zanzotto, 2001; Pitteri, 1985), graphene's lattice belong to a special category of multilattices: it is a hexagonal 2-lattice. The unit cell for all possible plane 2-lattices is given in Fadda and Zanzotto (2000). The fact that graphene is at the discrete level a 2-lattice has some important consequences when scaling up to the continuum. The most important consequence is that the shift vector should be an independent argument at the continuum energy (Parry, 1978; Ericksen, 1970, 1979; Fadda and Zanzotto, 2000, 2001; Pitteri, 1984, 1985; Pitteri and Zanzotto, 2003). The shift vector is the vector connecting the two simple hexagonal lattices that constitute the hexagonal 2-lattice of graphene (see also the Figures in Sfyris and Galiotis, in press; Sfyris et al., 2014a,b; Sfyris et al., in press). So, at the continuum level the energy should depend on the shift vector as well.

Lamdmark works on the continuum modeling of graphene stem from the fundamental work of Lee et al. (2008) who use a nanoidentation experiment in an atomic force microscope to measure the elastic properties and intrinsic strength of graphene. Using second order elasticity these authors evaluate Young's modulus, the second order elastic constant as well as graphene's breaking strength. Their analysis model graphene as an isotropic body in one dimension, due to symmetry in the loading. Generalization of their approach to two dimensions is done by Cadelano et al. (2009). These authors view graphene as an isotropic body and they utilize an energy cubic in strains (second order elasticity in words of Murnaghan (1951) and Rivlin (1963)). Utilizing tight-binding atomistic simulations they calculate Young's modulus, Poisson ratio as well as higher order constants for graphene. While interesting and novel their approach is, it lacks the treatment of bending effects. It also model graphene as an isotropic body; dependence on the zigzag and the armchair direction is not incorporated to the constitutive law through dependence on a structural tensor. Fifth order models for graphene are presented by Wei et al. (2009). These authors utilize an energy that depends on strains of the fifth order. Using density functional theory for simple loading histories they evaluate higher order constants for graphene. Their approach does not include bending effects neither anisotropy; graphene is modeled as an isotropic body.

Compared to these fundamental and interesting works, our line of work for modeling graphene as a 2-lattice (Sfyris and Galiotis, in press; Sfyris et al., 2014a,b; Sfyris et al., in press) add novelty in three levels: a. we include bending effects into our analysis by dependence of the energy on the curvature tensor, b. symmetries of graphene are properly taken into account starting from the discrete picture and passing consistently to the continuum using the structural tensor in line with the classical theories of invariants of nonlinear elasticity, c. our analysis is devoid of the endless Taylor expansion of the energy the abovementioned works utilize: evaluating the invariants we find the exact number of material parameters for a most generic energy describing the material at hand. To all these we add that graphene is a monoatomic 2-lattice and not a simple lattice that almost all works in literature assume. Thus, at the continuum energy the shift vector should be taken into account in line with well established theories of multilattices (see e.g. Chapter 11 of Pitteri and Zanzotto (2003)).

In the literature there are many works related with thin film/-substrate interactions, from the theoretical point of view. We refer to the paper by Mishnaevsky and Gross (2005) for a concise review of this topic as well as to its numerous references. We draw particular attention to the fundamental paper by Huang (2005). There, the substrate behave viscoelastically while for the thin film the von-Karman assumptions are adopted. Using plane strain analysis and the standard Laplace transformation method for converting a viscoelastic problem to an elastic one, the author solve the viscoelastic problem of the substrate. The effect of the thin film is present on the boundary condition of the equations governing the bulk material.

Another interesting study is the approach of Cao and Hutchinson (2012) who adopt a neo-Hookean expression for the energy of the film as well as for the substrate in order to study the effect of the pre-stretch of the substrate. Fried and Todres (2005), study the effect of curvature and residual stress to the buckling of a half space with free surface near a contactor. They assume that the bulk and the boundary body are made of the same material and use the geometrical symmetry to reduce the problem to one dimension only. It is important to note that these authors introduce van der Waals effects in their analysis. The effect of the surface tension of a free surface on the bulk material is studied by Wang et al. (2010) who also assume that the free surface and the bulk body are made of the same material. The case of partial delamination of the thin film from the substrate is an undesirable phenomenon which appears frequently in the manufacturing process. Bedrossian and Kohn (2015) lay down a specific expression for the displacement function that describe partial delamination in the form of a blister.

The main novelty of the present contribution lies on the fact that we take into account the presence of the substrate on closed form solutions related with simple loadings. This is done for the case where graphene and substrate are perfectly bonded and also for the case where delamination take place. Additionally, we retain throughout the analysis terms related with residual strains for both the thin film and the substrate. We adopt the field equations as reported by Chhapadia et al. (2011). These are the momentum and the moment of momentum equations for the thin film (graphene) in the absence of body forces and inertia. The effect of the substrate enter through terms present in these equations. To these equations one should add the equation ruling the shift vector (Parry, 1978; Ericksen, 1970, 1979; Fadda and Zanzotto, 2000, 2001; Pitteri, 1984, 1985; Pitteri and Zanzotto, 2003) since graphene is a multilattices.

To bring our framework closer to more applied approaches and to give a rough order of magnitude for plotting purposes, we present the mean stress–strain diagrams for the axial tension test and the simple shear problem. For the substrate we make three different assumptions corresponding to three common materials used as substrate: Polyethylene terephthalate (PET), Polymethyl methacrylate (PMMA) and Polydimethylsiloxane (PDMS). In the mathematical model these are introduced through their Lame constants, λ, μ. Being aware that these polymeric substrate's behave in a viscoelastic manner, we assume the viscous response to be negligible, since we have in mind experiments with slow rate such as those in Androulidakis et al. (2014).

For graphene we adopt the linear framework of Sfyris et al. (2014b), so the whole theory is confined to geometrical and

Please cite this article in press as: Sfyris, D., et al. Graphene resting on substrate: Closed form solutions for the perfect bonding and the delamination case. Int. J. Solids Struct. (2015), http://dx.doi.org/10.1016/j.ijsolstr.2015.06.024

material linearities for both film and substrate. For this linear modeling the in-surface material constants are four: $c_1,\ c_2,\ c_5,\ c_9$. In a recent work (Sfyris et al., submitted for publication) we evaluate them using molecular mechanics calculations. There (Sfyris et al., submitted for publication) we focus on graphene's unit cell and distinguish between the measured length of the shift vector and the length of the lattice vectors. Then we apply a tensional strain and evaluate the radial distribution diagram describing length changes due to the applied loading for carbon–carbon connections. At zero strain level we find two peaks on the radial distribution diagram: one corresponding to the equal length of the lattice vectors (approximately 0.242 nm) while the other peak correspond to the shift vector (approximately 0.140 nm). As strain is gradually applied, we find that these two peaks split into two new peaks each. To these four peaks we correspond at the continuum level the four required material parameters. Comparison with standard literature render then the values $(c_1, c_2, c_5, c_9) = (1.102, 1.534, 3.117, -12.07)$ TPa. These values for graphene together with the substrate's material parameters are used in Section 3 to produce the mean stress–strain diagrams for the axial strain and the simple shear problem.

Throughout our analysis we distinguish between two displacement fields: one for the film and the second for the substrate and study two groups of solutions: one where the bonding is perfect and one where delamination take place. For the perfect bonding case we divide into two categories: one where only in-surface motions are considered and another where we treat in-surface motions together with out-of-surface motions.

For the perfect bonding case we study biaxial tension/compression as well as shear loading.We find the components of the shift vector by solving the equations ruling the shift vector. We then substitute this expression for the shift vector components to the momentum equation. This way we obtain conditions that the field of the internal strains, the strain constants and the material parameters should satisfy in order biaxial tension/compression and simple shear to be solutions for all equilibrium equations. We particularize to the axial strain problem and produce the mean stress–strain curves for all stress components. Taking three different choices for the substrate we highlight the role a stiffer or softer substrate has in the mean stress components. A similar analysis is done for the simple shear problem. For both problems we also take into account how a field of in-surface internal strain affect the mean stress–strain curves.

For the out-of-surface case we use a semi-inverse method. Motivated by the work of Puntel et al. (2011) we assume a specific form for the out-of-surface displacement. This displacement is the product of a wave-like function with an unknown function, f, which turns out to be the basic unknown for the problem at hand. Solving the equations ruling the shift vector we evaluate the shift vector components as a function of all other measures: the internal strains, the in-surface strain and curvature. We substitute these expressions to the momentum equation to obtain an equation for the unknown function f. We find conditions in order the momentum equation to be explicitly solvable for the unknown function f. These conditions are constraints that the field of the internal strains, the strain constants and the material parameters should satisfy.

Distinguishing film's displacement from the displacement of the substrate, we introduce delamination in our analysis. Motivated by the work of Bedrossian and Kohn (2015) we make a specific assumption for the delamination function. This function has two parts: one trivial describing the perfect bonding areas and one non-trivial describing the delaminated areas. The delaminated part is described by a displacement which is a product of a wave-like function together with an unknown function, g. We find the shift vector components solving the equations ruling the shift vector and substitute them to the momentum equation. This way we obtain an equation for the unknown function g, which we determine explicitly under some conditions. These conditions are constraints that the field of the internal strains, the strain constant and the material parameters should satisfy. This procedure is done twice: one for the perfect bonding areas and one for the delaminted areas.

The paper is organized as follows. Section 2 give a short reminder of the constitutive modeling of graphene as a hexagonal 2-lattice (Sfyris and Galiotis, in press; Sfyris et al., 2014a,b; Sfyris et al., in press). In the same section, we also give the constitutive modeling of the substrate and lay down the field equations in terms of stress and strain quantities. Section 3 treats the in-surface perfect bonding case. We apply biaxial tension/compression to the film/substrate system and evaluate the shift vector components by solving the equation ruling the shift vector. We then substitute them to the momentum equation to obtain constraints that should be satisfied by the field of the internal strains, the material parameters and the strain constants, in order the equilibrium equations to be satisfied. We then particularize to the case of axial strain and produce the mean stress–strain diagrams for three different choices for the substrate's. The same procedure is done for the simple shear case. We also examine the role a field of internal strains has in the mean stress–strain diagrams.

Section 4 treat out-of-surface motions of perfectly bonded surfaces; we find specific solutions for the out-of-surface motions under certain conditions. These are conditions that the strain constants, the field of internal strains and the material parameters of the substrate should satisfy in order all field equations to be satisfied trivially. Section 5 studies the debonding case. By making a suitable assumption for the film's displacement that now differ from the substrate's one, we find specific solutions under certain conditions. These again are conditions that the field of the internal strains, the loading constants and the material moduli should satisfy in order all field equations to be satisfied trivially. These conditions then guarantee that the delamination function chosen is a solution for the problem at hand. Section 6, conclude the paper with discussion of the results.

2. Mathematical prerequisites

Graphene is modeled as a hexagonal 2-lattice, in line with previous approaches on relevant topics (Sfyris and Galiotis, in press; Sfyris et al., 2014a,b; Sfyris et al., in press). The need for viewing graphene as a multilattice stem from the fact that graphene's lattice cannot be seen as a Bravais simple lattice. In standard terminology of applied crystallography (Fadda and Zanzotto, 2000, 2001; Pitteri, 1985), graphene's lattice belong to a special category of multilattices: it is a hexagonal 2-lattice. The unit cell for all possible plane 2-lattices is given in Fadda and Zanzotto (2000). The fact that graphene is at the discrete level a 2-lattice has some important consequences when scaling up to the continuum. The most important consequence is that the shift vector should be an independent argument at the continuum energy (Parry, 1978; Ericksen, 1970, 1979; Fadda and Zanzotto, 2000, 2001; Pitteri, 1984, 1985; Pitteri and Zanzotto, 2003). The shift vector is the vector connecting the two simple hexagonal lattices that constitute the hexagonal 2-lattice of graphene (see Figs. in Sfyris and Galiotis, in press; Sfyris et al., 2014a,b). So, at the continuum level the energy should depend on the shift vector as well.

For the geometrical and materially linear case graphene's energy depend on an in-surface strain measure, the curvature tensor and the shift vector. Dependence on the curvature tensor is motivated by the work of Steigmann and Ogden (1999). Dependence on the shift vector result from well established

Please cite this article in press as: Sfyris, D., et al. Graphene resting on substrate: Closed form solutions for the perfect bonding and the delamination case. Int. J. Solids Struct. (2015), http://dx.doi.org/10.1016/j.ijsolstr.2015.06.024

theories of multilattices (Parry, 1978; Ericksen, 1970, 1979; Fadda and Zanzotto, 2000; Fadda and Zanzotto, 2001; Pitteri, 1984, 1985; Pitteri and Zanzotto, 2003). So, all in all, graphene's elastic energy has the form (Sfyris et al., 2014b)

$$\begin{aligned} W(\mathbf{e},\mathbf{b},\mathbf{p}) = &\frac{1}{2}C^1_{ijkl}e^{0\,f}_{ij}e^{0\,f}_{kl} + \frac{1}{2}C^2_{ij}p^0_i p^0_j + \frac{1}{2}C^3_{ijk}e^{0\,f}_{ij}p^0_k \\ &+ \frac{1}{2}C^4_{ijkl}b^{0\,f}_{ij}b^{0\,f}_{kl} + \frac{1}{2}C^5_{ijkl}e^{0\,f}_{ij}b^{0\,f}_{kl} + \frac{1}{2}C^6_{ijk}b^{0\,f}_{ij}p^0_k \\ &+ \frac{1}{2}C^1_{ijkl}e^f_{ij}e^f_{kl} + \frac{1}{2}C^2_{ij}p_i p_j + \frac{1}{2}C^3_{ijk}e^f_{ij}p_k + \frac{1}{2}C^4_{ijkl}b^f_{ij}b^f_{kl} \\ &+ \frac{1}{2}C^5_{ijkl}e^f_{ij}b^f_{kl} + \frac{1}{2}C^6_{ijk}b^f_{ij}p_k, \end{aligned} \tag{1}$$

where $e^f_{ij} = \frac{1}{2}(u^f_{i,j} + u^f_{j,i})$ is the in-surface strain measure of the film, $\mathbf{u}^f$ is the displacement of the film, $\mathbf{b}^f$ is film's curvature, while $\mathbf{p}$ is graphene's shift vector. Tensors $\mathcal{C}^i$, $i = 1,\dots,6$ are related with the material parameters of the problem at hand (see Sfyris et al., 2014b).

Geometrical nonlinearities are absent, since we neglect terms of the form $u^f_{i,j}u^f_{i,j}$ on e^f_{ij}. Material linearities are expressed by the fact that graphene's energy is a quadratic function of $\mathbf{e}^f$, $\mathbf{b}^f$, $\mathbf{p}$ and combinations of them. Quantities related with residual/internal strains are denoted by a superposed 0. These are the residual in-surface strain in the film, e^{0f}_{ij}, the out-of-surface residual strains measured by the term $\mathbf{b}^{0\,f}$: the residual part of the curvature. Term $\mathbf{p}^0$ is related to residual strains from the shift vector dependence.

The stress tensor, the couple stress tensor and the stress-like quantity related with the shift vector, for the thin film read (Sfyris et al., 2014b) respectively

$$\begin{aligned} \sigma^f_{ij} &= \frac{\partial W}{\partial e^f_{ij}} \\ &= C^1_{ijkl}e^{0\,f}_{kl} + C^3_{ijk}p^0_k + C^5_{ijkl}b^{0\,f}_{kl} + C^1_{ijkl}e^f_{kl} + C^3_{ijk}p_k + C^5_{ijkl}b^f_{kl}, \end{aligned} \tag{2}$$

$$\begin{aligned} m^f_{ij} &= \frac{\partial W}{\partial b^f_{ij}} \\ &= C^4_{ijkl}b^{0\,f}_{kl} + C^5_{ijkl}e^{0\,f}_{kl} + C^6_{ijk}p^0_k + C^4_{ijkl}b^f_{kl} + C^5_{ijkl}e^f_{kl} + C^6_{ijk}p_k, \end{aligned} \tag{3}$$

$$\frac{\partial W}{\partial p_i} = C^2_{ij}p^0_j + C^3_{ijk}e^{0\,f}_{jk} + C^6_{ijk}b^{0\,f}_{jk} + C^2_{ij}p_j + C^3_{ijk}e^f_{jk} + C^6_{ijk}b^f_{jk}. \tag{4}$$

Ultimately these expressions render for the components of the stress tensor

$$\begin{aligned} \sigma^f_{11} = &c_1e^{0\,f}_{11} + c_2e^{0\,f}_{22} + c_3b^{0\,f}_{11} + c_4b^{0\,f}_{22} - c_5p^0_2 + c_1e^f_{11} + c_2e^f_{22} \\ &+ c_3b^f_{11} + c_4b^f_{22} - c_5p_2, \end{aligned} \tag{5}$$

$$\begin{aligned} \sigma^f_{22} = &c_2e^{0\,f}_{11} + c_1e^{0\,f}_{22} + c_4b^{0\,f}_{11} + c_3b^{0\,f}_{22} + c_5p^0_2 + c_2e^f_{11} + c_1e^f_{22} \\ &+ c_4b^f_{11} + c_3b^f_{22} + c_5p_2, \end{aligned} \tag{6}$$

$$\begin{aligned} \sigma^f_{12} = &\frac{c_1 - c_2}{2}e^{0\,f}_{12} + \frac{c_3 - c_4}{2}b^{0\,f}_{12} - 2c_5p^0_1 + \frac{c_1 - c_2}{2}e^f_{12} \\ &+ \frac{c_3 - c_4}{2}b^f_{12} - 2c_5p_1. \end{aligned} \tag{7}$$

For the couple stress tensor we obtain

$$\begin{aligned} m^f_{11} = &c_6b^{0\,f}_{11} + c_7b^{0\,f}_{22} + c_3e^{0\,f}_{11} + c_4e^{0\,f}_{22} - c_8p^0_2 + c_6b^f_{11} + c_7b^f_{22} \\ &+ c_3e^f_{11} + c_4e^f_{22} - c_8p_2, \end{aligned} \tag{8}$$

$$\begin{aligned} m^f_{22} = &c_7b^{0\,f}_{11} + c_6b^{0\,f}_{22} + c_4e^{0\,f}_{11} + c - 3e^{0\,f}_{22} + c_8p^0_2 + c_7b^f_{11} \\ &+ c_6b^f_{22} + c_4e^f_{11} + c - 3e^f_{22} + c_8p_2, \end{aligned} \tag{9}$$

$$\begin{aligned} m^f_{12} = &\frac{c_6 - c_7}{2}b^{0\,f}_{12} + \frac{c_3 - c_4}{2}e^{0\,f}_{12} - 2c_8p^0_1 + \frac{c_6 - c_7}{2}b^f_{12} \\ &+ \frac{c_3 - c_4}{2}e^f_{12} - 2c_8p_1. \end{aligned} \tag{10}$$

For the stress-like quantities related with the shift vector we find

$$\frac{\partial W}{\partial p_1} = c_9p^0_1 - 2c_5e^{0\,f}_{12} - 2c_8b^{0\,f}_{12} + c_9p_1 - 2c_5e^f_{12} - 2c_8b^f_{12}, \tag{11}$$

$$\begin{aligned} \frac{\partial W}{\partial p_2} = &c_9p^0_2 - c_5e^{0\,f}_{11} + c_5e^{0\,f}_{22} - c_8b^{0\,f}_{11} + c_8b^{0\,f}_{22} + c_9p_2 - c_5e^f_{11} \\ &+ c_5e^f_{22} - c_8b^f_{11} + c_8b^f_{22}. \end{aligned} \tag{12}$$

In the above equations constants c_i, $i = 1,\dots,9$ correspond to the material parameters of graphene when it is modeled as a hexagonal 2-lattice in the linear case (see Sfyris et al., 2014b).

For this linear modeling the in-surface material constants are four: c_1, c_2, c_5, c_9. In a recent work (Sfyris et al., submitted for publication) we evaluate them using molecular mechanics calculations. There (Sfyris et al., submitted for publication) we focus on graphene's unit cell and distinguish between the measured length of the shift vector and the length of the lattice vectors. Then we apply a tensional strain and evaluate the radial distribution diagram describing length changes due to the applied loading for carbon–carbon connections. At zero strain level we find two peaks on the radial distribution diagram: one corresponding to the equal length of the lattice vectors (approximately 0.242 nm) while the other peak correspond to the shift vector (approximately 0.140 nm). As strain is gradually applied, we find that these two peaks split into two new peaks each. To these four peaks we correspond, at the continuum level, the four required material parameters. Comparison with standard literature render then the values $(c_1, c_2, c_5, c_9) = (1.102, 1.534, 3.117, -12.07)$ TPa.

On the other hand, the substrate is assumed to behave as a linear isotropic elastic material. Thus the constitutive law read

$$\sigma^b_{ij} = \lambda e^{0\,b}_{kk}\delta_{ij} + 2\mu e^{0\,b}_{ij} + \lambda e^b_{kk}\delta_{ij} + 2\mu e^b_{ij}, \tag{13}$$

where $e^b_{ij} = \frac{1}{2}\left(u^b_{i,j} + u^b_{j,i}\right)$ is the strain tensor for the substrate and $\mathbf{u}^b$ is the displacement of the bulk material (the substrate). λ, μ are the Lame constants of the substrate. We disregard viscous effects, since we have in mind experiments with slow rate such as the one's performed in Androulidakis et al. (2014). $\mathbf{e}^{0\,b}$ denotes the internal strain field the substrate has.

From the above analysis one observe that essentially into the mathematical framework there are two displacement fields: one for the thin film ($\mathbf{u}^f$) and one for the substrate ($\mathbf{u}^b$). In the case of perfect bonding these two quantities are equal. When delamination take place they differ in some areas; these are the areas where debonding occur. It is also worth mentioning that $\mathbf{u}^f$ has components u^f_1, u^f_2; namely it is a two dimensional quantity. Out-of-surface motions for the film are described through the term $\mathbf{b}^f$: the curvature tensor (see Sfyris et al., 2014a,b). On the other hand, $\mathbf{u}^b$ is a three dimensional quantity; it has three components. Deformations out of the bounding surface of the substrate are therefore introduced into the mathematical framework by u^b_3. Both $\mathbf{u}^f$ and $\mathbf{u}^b$ are parametrized by two surface coordinates Θ^α, $\alpha = 1, 2$ (see Sfyris et al., 2014b).

The field equations are then (Chhapadia et al., 2011)

$$\sigma^b_{ij}n^b_j + \sigma^f_{ij,j} = 0, \tag{14}$$

$$\epsilon_{mn}u^b_m n^b_q \sigma^b_{nq}e_i + m^f_{ij,j} - (\epsilon_{mn}\sigma^f_{mi}u^f_n e_p)_{,p} = 0, \tag{15}$$

$$\sigma^b_{ij}n^b_j + \frac{\partial W}{\partial p_i} = 0. \tag{16}$$

Please cite this article in press as: Sfyris, D., et al. Graphene resting on substrate: Closed form solutions for the perfect bonding and the delamination case. Int. J. Solids Struct. (2015), http://dx.doi.org/10.1016/j.ijsolstr.2015.06.024

Eq. (14) is the momentum equation in the absence of body forces and inertia; it is the balance of forces for the surface. Eq. (15) is the moment of momentum equation in the absence of inertia and body couples. From the physical point of view it describe the couple balance in the surface. Eq. (16) express that the shift vector adjust so as equilibrium is reached (Ericksen, 1979; Pitteri and Zanzotto, 2003). It is interesting here to note that the presence of the out-of-surface unit normal, $\mathbf{n}^b$, explicitly in the field equations lead to dependence of the solutions in this field.

Using Eqs. (5)–(7) and (13) on Eq. (14) for the first of the momentum equation we obtain

$$\begin{aligned}&\lambda(e^{0\,b}_{11}+e^{0\,b}_{22}+e^{0\,b}_{33})n^b_1+2\mu e^{0\,b}_{11}n^b_1+2\mu e^{0\,b}_{12}n^b_2+2\mu e^{0\,b}_{13}n^b_3+\lambda u^b_{1,1}n^b_1\\&+\lambda u^b_{2,2}n^b_1+2\mu u^b_{1,1}n^b_1+\mu(u^b_{1,2}+u^b_{2,1})n^b_2+\mu u^b_{3,1}n^b_3+c_1e^{0\,f}_{11,1}\\&+c_2e^{0\,f}_{22,1}+c_3b^{0\,f}_{11,1}+c_4b^{0\,f}_{22,1}-c_5p^0_{2,1}+\frac{c_1-c_2}{2}e^{0\,f}_{12,2}\\&+\frac{c_3-c_4}{2}b^{0\,f}_{12,2}-2c_5p^0_{1,2}+c_1u^f_{1,11}+c_2u^f_{2,21}+c_3b^f_{11,1}+c_4b^f_{22,1}\\&-c_5p_{2,1}+\frac{c_1-c_2}{4}(u^f_{1,22}+u^f_{2,12})+\frac{c_3-c_4}{2}b^f_{12,2}-2c_5p_{1,2}=0.\end{aligned}\tag{17}$$

For the second equation of momentum we take

$$\begin{aligned}&\lambda(e^{0\,b}_{11}+e^{0\,b}_{22}+e^{0\,b}_{33})n^b_2+2\mu e^{0\,b}_{21}n^b_1+2\mu e^{0\,b}_{22}n^b_2+2\mu e^{0\,b}_{23}n^b_3\\&+\lambda(u^b_{1,1}+u^b_{2,2})n^b_2+\mu(u^b_{1,2}+u^b_{2,1})n^b_1+2\mu u^b_{2,2}n^b_2+\mu u^b_{3,2}n^b_3\\&+c_2e^{0\,f}_{11,2}+c_1e^{0\,f}_{22,2}+c_4b^{0\,f}_{11,2}+c_3b^{0\,f}_{22,2}+c_5p^0_{2,2}+\frac{c_1-c_2}{2}e^{0\,f}_{12,1}\\&+\frac{c_3-c_4}{2}b^{0\,f}_{12,1}-2c_5p^0_{1,1}+\frac{c_1-c_2}{4}(u^f_{1,21}+u^f_{2,11})+\frac{c_3-c_4}{2}b^f_{12,1}\\&-2c_5p_{1,1}+c_2u^f_{1,12}+c_1u^f_{2,22}+c_4b^f_{11,2}+c_3b^f_{22,2}+c_5p_{2,2}=0.\end{aligned}\tag{18}$$

Using Eqs. (11)–(13) on Eq. (16) for the first equation ruling the shift vector we evaluate

$$\begin{aligned}&\lambda(e^{0\,b}_{11}+e^{0\,b}_{22}+e^{0\,b}_{33})n^b_1+2\mu e^{0\,b}_{11}n^b_1+2\mu e^{0\,b}_{12}n^b_2+2\mu e^{0\,b}_{13}n^b_3\\&+\lambda u^b_{1,1}n^b_1+\lambda u^b_{2,2}n^b_1+2\mu u^b_{1,1}n^b_1+c_9p^0_1-2c_5e^{0\,f}_{12}-2c_8b^{0f}_{12}\\&+\mu(u^b_{1,2}+u^b_{2,1})n^b_2+\mu u^b_{3,1}n^b_3+c_9p_1-c_5(u^f_{1,2}+u^f_{2,1})-2c_8b^f_{12}=0.\end{aligned}\tag{19}$$

For the second equation ruling the shift vector we find

$$\begin{aligned}&\lambda(e^{0\,b}_{11}+e^{0\,b}_{22}+e^{0\,b}_{33})n^b_2+2\mu e^{0\,b}_{21}n^b_1+2\mu e^{0\,b}_{22}n^b_2+2\mu e^{0\,b}_{23}n^b_3\\&+\lambda(u^b_{1,1}+u^b_{2,2})n^b_2+\mu(u^b_{1,2}+u^b_{2,1})n^b_1+c_9p^0_2-c_5e^{0\,f}_{11}-c_5e^{0\,f}_{22}\\&-c_8b^{0\,f}_{11}+c_8b^{0\,f}_{22}+2\mu u^b_{2,2}n^b_2+\mu u^b_{3,2}n^b_3+c_9p_2-c_5u^f_{1,1}+c_5u^f_{2,2}\\&-c_8b^f_{11}+c_8b^f_{22}=0.\end{aligned}\tag{20}$$

In a similar fashion using Eqs. (5)–(10) to Eq. (15) one may obtain the moment of momentum equation in terms of the displacement fields. Since this equation is not explicitly used in later Sections we refrain from writing it down, but we stress that one can obtain this equation in a straightforwrd manner.

Next sections utilize the above equations by making suitable assumptions for the displacement field of the film and the substrate. Essentially, there are two cases studied: first, the case of perfect bonding between the film and the substrate, and second, the case of debonding between them. In the case of perfect bonding, i.e., when $\mathbf{u}^f=\mathbf{u}^b$, we distinguish between a case without out-of-surface motion and a case where out-of-surface motion take place. When there are no out-of-surface motions we need not use the moment of momentum equation neither the curvature tensor comes into play. We also treat the case where delamination occur; in this case the displacement of the film differs from the one of the bulk in the delaminated areas.

3. In-surface motions-perfect bonding

Since we restrict ourselves to in-surface motions only we set film's curvature equal. Also, for the component u^b_3 we have that it is zero, since this describe out-of-surface motions of the bulk material. Perfect bonding means $\mathbf{u}^f=\mathbf{u}^b$. We study biaxial tension/compression and simple shear for the case of perfect bonding using a semi-inverse method. We assume the form the displacement has and evaluate all other quantities in order the field equations to be satisfied trivially.

3.1. Biaxial tension/compression

Following our previous works (Sfyris et al., 2014a,b) we introduce biaxial tension/compression by assuming for the displacement components ($\mathbf{u}^b=\mathbf{u}^f=\mathbf{u}$)

$$u_1=\epsilon_1\Theta^1,\quad u_2=\epsilon_2\Theta^2.\tag{21}$$

When $\epsilon_i>1$ then the material is under tension in the i-direction. When $\epsilon_i<1$ the material is under compression in this direction. Then, the first equation for the shift vector, Eq. (19), can be solved in terms of p_1 to give

$$\begin{aligned}p_1=\frac{1}{c_9}\big[&-\lambda\epsilon_1n^b_1-\lambda\epsilon_2n^b_2-2\mu\epsilon_1n^b_1-\lambda(e^{0\,b}_{11}+e^{0\,b}_{22})n^b_1-2\mu e^{0\,b}_{11}n^b_1\\&-2\mu e^{0\,b}_{12}n^b_2-c_9p^0_1+2c_5e^{0\,f}_{12}\big].\end{aligned}\tag{22}$$

The second equation ruling the shift vector, Eq. (20), render

$$\begin{aligned}p_2=\frac{1}{c_9}[&-\lambda(\epsilon_1+\epsilon_2)n^b_2-2\mu\epsilon_2n^b_2+c_5\epsilon_1-c_5\epsilon_2-\lambda(e^{0\,b}_{11}+e^{0\,b}_{22})n^b_2\\&-2\mu e^{0\,b}_{21}n^b_1-2\mu e^{0\,b}_{22}n^b_2-c_9p^0_2+c_5e^{0\,f}_{11}+c_5e^{0\,f}_{22}].\end{aligned}\tag{23}$$

Substituting Eqs. (22) and (23) to the first of the momentum equation, Eq. (17), we take

$$\begin{aligned}&\lambda(e^{0\,b}_{11}+e^{0\,b}_{22})n^b_1+2\mu e^{0\,b}_{11}n^b_1+2\mu e^{0\,b}_{12}n^b_2+\lambda\epsilon_1n^b_1+\lambda\epsilon_2n^b_1+2\mu\epsilon_1n^b_1\\&+c_1e^{0\,f}_{11,1}+c_2e^{0\,f}_{22,1}+c_3b^{0\,f}_{11,1}+c_4b^{0\,f}_{22,1}-c_5p^0_{2,1}+\frac{c_1-c_2}{2}e^{0\,f}_{12,2}\\&+\frac{c_3-c_4}{2}b^{0\,f}_{12,2}-2c_5p^0_{1,2}+\frac{c_5}{c_9}[\lambda(\epsilon_1+\epsilon_2)n^b_2+2\mu\epsilon_2n^b_2]_{,1}\\&+2\frac{c_5}{c_9}[\lambda\epsilon_1n^b_1+\lambda\epsilon_2n^b_2+2\mu\epsilon_1n^b_1]_{,2}+\frac{c_5}{c_9}[\lambda(e^{0\,b}_{11}+e^{0\,b}_{22})n^b_2\\&+2\mu e^{0\,b}_{21}n^b_1+2\mu e^{0\,b}_{22}n^b_2+c_9p^0_2-c_5e^{0\,f}_{11}-c_5e^{0\,f}_{22}]_{,1}\\&+2\frac{c_5}{c_9}[+\lambda(e^{0\,b}_{11}+e^{0\,b}_{22})n^b_1+2\mu e^{0\,b}_{11}n^b_1\\&+2\mu e^{0\,b}_{12}n^b_2+c_9p^0_1-2c_5e^{0\,f}_{12}]_{,2}=0.\end{aligned}\tag{24}$$

The second equation of momentum, Eq. (18), render then

$$\begin{aligned}&\lambda(e^{0\,b}_{11}+e^{0\,b}_{22})n^b_2+2\mu e^{0\,b}_{21}n^b_1+2\mu e^{0\,b}_{22}n^b_2+\lambda(\epsilon_1+\epsilon_2)n^b_2\\&+2\mu\epsilon_2n^b_2+c_2e^{0\,f}_{11,2}+c_1e^{0\,f}_{22,2}+c_4b^{0\,f}_{11,2}+c_3b^{0\,f}_{22,2}+c_5p^0_{2,2}\\&+\frac{c_1-c_2}{2}e^{0\,f}_{12,1}+\frac{c_3-c_4}{2}b^{0\,f}_{12,1}-2c_5p^0_{1,1}+2\frac{c_5}{c_9}[\lambda\epsilon_1n^b_1+\lambda\epsilon_2n^b_2\\&+2\mu\epsilon_1n^b_1]_{,1}-\frac{c_5}{c_9}[\lambda(\epsilon_1+\epsilon_2)n^b_2+2\mu\epsilon_2n^b_2]_{,2}\\&+2\frac{c_5}{c_9}\Big[\lambda(e^{0\,b}_{11}+e^{0\,b}_{22})n^b_1+2\mu e^{0\,b}_{11}n^b_1+2\mu e^{0\,b}_{12}n^b_2+c_9p^0_1-2c_5e^{0\,f}_{12}\Big]_{,1}\\&+\frac{c_5}{c_9}[-\lambda(e^{0\,b}_{11}+e^{0\,b}_{22})n^b_2-2\mu e^{0\,b}_{21}n^b_1-2\mu e^{0\,b}_{22}n^b_2-c_9p^0_2\\&+c_5e^{0\,f}_{11}+c_5e^{0\,f}_{22}]_{,2}=0.\end{aligned}\tag{25}$$

The equations of momentum, Eqs. (24) and (25), render conditions that the field of internal strains, the strain constants, ϵ_1, ϵ_2, the vector $\mathbf{n}^b$ and the material parameters, c_1, c_2, c_5, c_9, λ, μ, should satisfy in order Eq. (21) to be a solution for all field equations.

Please cite this article in press as: Sfyris, D., et al. Graphene resting on substrate: Closed form solutions for the perfect bonding and the delamination case. Int. J. Solids Struct. (2015), http://dx.doi.org/10.1016/j.ijsolstr.2015.06.024

The constitutive laws for graphene at this case read

$$\sigma^f_{11} = c_1 e^{0\,f}_{11} + c_2 e^{0\,f}_{22} - c_5 p^0_2 + c_1\epsilon_1 + c_2\epsilon_2 - \frac{c_5}{c_9}[-\lambda(\epsilon_1+\epsilon_2)n^b_2 - 2\mu\epsilon_2 n^b_2 + c_5\epsilon_1 - c_5\epsilon_2 - \lambda(e^{0\,b}_{11} + e^{0\,b}_{22})n^b_2 - 2\mu e^{0\,b}_{21} n^b_1 - 2\mu e^{0\,b}_{22} n^b_2 - c_9 p^0_2 + c_5 e^{0\,f}_{11} + c_5 e^{0\,f}_{22}], \tag{26}$$

$$\sigma^f_{22} = c_2 e^{0\,f}_{11} + c_1 e^{0\,f}_{22} + c_5 p^0_2 + c_2\epsilon_1 + c_1\epsilon_2 + \frac{c_5}{c_9}[-\lambda(\epsilon_1+\epsilon_2)n^b_2 - 2\mu\epsilon_2 n^b_2 + c_5\epsilon_1 - c_5\epsilon_2 - \lambda(e^{0\,b}_{11} + e^{0\,b}_{22})n^b_2 - 2\mu e^{0\,b}_{21} n^b_1 - 2\mu e^{0\,b}_{22} n^b_2 - c_9 p^0_2 + c_5 e^{0\,f}_{11} + c_5 e^{0\,f}_{22}]; \tag{27}$$

$$\sigma^f_{12} = \frac{c_1 - c_2}{2} e^{0\,f}_{12} - 2c_5 p^0_1 - 2\frac{c_5}{c_9}[-\lambda\epsilon_1 n^b_1 - \lambda\epsilon_2 n^b_2 - 2\mu\epsilon_1 n^b_1 - \lambda(e^{0\,b}_{11} + e^{0\,b}_{22})n^b_1 - 2\mu e^{0\,b}_{11} n^b_1 - 2\mu e^{0\,b}_{12} n^b_2 - c_9 p^0_1 + 2c_5 e^{0\,f}_{12}]. \tag{28}$$

For the particular case where the applied strain is axial, namely when $\epsilon_2 = 1$, and there are no internal strains, we obtain for the components of the shift vector from Eqs. (22) and (23)

$$p_1 = \frac{1}{c_9}[-\lambda\epsilon_1 n^b_1 - 2\mu\epsilon_1 n^b_1], \tag{29}$$

$$p_2 = \frac{1}{c_9}[-\lambda\epsilon_1 n^b_2 + c_5\epsilon_1 - c_5]. \tag{30}$$

The constitutive expression for the stress tensor components, Eqs. (26)–(28), then simplify to

$$\sigma^f_{11} = c_1\epsilon_1 - \frac{c_5}{c_9}[-\lambda\epsilon_1 n^b_2 + c_5\epsilon_1], \tag{31}$$

$$\sigma^f_{22} = c_2\epsilon_1 + \frac{c_5}{c_9}[-\lambda\epsilon_1 n^b_2 + c_5\epsilon_1], \tag{32}$$

$$\sigma^f_{12} = -2\frac{c_5}{c_9}[-\lambda\epsilon_1 n^b_1 - 2\mu\epsilon_1 n^b_1]. \tag{33}$$

These are the pointwise expressions for the components of the stress tensor, namely $\sigma^f_{ij} = \sigma^f_{ij}(\Theta^1, \Theta^2)$. We notice that the inhomogeneity of these quantities stem from the explicit dependence on $\mathbf{n}^b$, the outward unit normal of the substrate. We now assume that $\mathbf{n}^b$ is the outward unit normal to a plane, namely, we assume that the film is a plane. So, we take $\mathbf{n}^b = (\Theta^1, \Theta^2, 1)$, such that $(\Theta^1)^2 + (\Theta^2)^2 + 1 = 1$ and further assume that $0 \leqslant \Theta^1 \leqslant 1,\ 0 \leqslant \Theta^2 \leqslant 1$. We now define the mean stress tensor components as

$$\sigma^{f\ mean}_{ij} = \int_0^1 \int_0^1 \sigma^f_{ij}(\Theta^1, \Theta^2) d\Theta^1 d\Theta^2. \tag{34}$$

The introduction of the mean stress of Eq. (34) rules out the inhomogeneity of the stress components. So, for the components of the mean stress we obtain

$$\sigma^{f\ mean}_{11} = c_1\epsilon_1 - \frac{c_5}{c_9}\left[-\frac{\lambda}{2}\epsilon_1 + c_5\epsilon_1\right], \tag{35}$$

$$\sigma^{f\ mean}_{22} = c_2\epsilon_1 + \frac{c_5}{c_9}\left[-\frac{\lambda}{2}\epsilon_1 + c_5\epsilon_1\right], \tag{36}$$

$$\sigma^{f\ mean}_{12} = -2\frac{c_5}{c_9}\left[-\frac{\lambda}{2}\epsilon_1 - 2\frac{\mu}{2}\epsilon_1\right]. \tag{37}$$

Fig. 1 give the mean stress–strain diagrams for the mean stress components $\sigma^{f\ mean}_{ij}$ from Eqs. (35)–(37). For producing all curves in this Section we assume the values $(c_1, c_2, c_5, c_9) = (1.102, 1.534, 3.117, -12.07)$ TPa for the material parameters of graphene (Sfyris et al., submitted for publication). For the Lame constants of the substrate we use the pairs $(\lambda, \mu) = (0.00259, 0.00111)$ TPa for the PMMA, $(\lambda, \mu) = (0.00429, 0.00107)$ TPa for PET and $(\lambda, \mu) = (9.8 \times 10^{-6}, 2 \times 10^{-7})$ TPa. Certainly, the PDMS is much softer that the PMMA and the PET (www.mit.edu/6.777/matprops).

Fig. 1(a) plot $\sigma^{f\ mean}_{11}$ versus ϵ_1; ϵ_1 is the measure of strain in % and all our diagrams are for $\epsilon_1 = 0$—1.6%. Fig. 1(b) plot $\sigma^{f\ mean}_{22}$ versus ϵ_1, while Fig. 1(c) plot $\sigma^{f\ mean}_{12}$ versus ϵ_1. For Fig. 1(a) and (b) we see that the effect of the substrate is negligible in the mean stress components $\sigma^{f\ mean}_{11}$, $\sigma^{f\ mean}_{22}$. Whether the substrate is stiff or soft does not affect $\sigma^{f\ mean}_{11}$, $\sigma^{f\ mean}_{22}$ significantly. This can be seen from Eqs. (35) and (36): the first and the third term are the dominant terms. These are terms resulting from graphene solely; the substrate is not present in them. The second term of Eqs. (35) and (36) is much smaller since the modulus of the substrate is much smaller than the in-plane material parameters of graphene. So, for $\sigma^{f\ mean}_{11}$, $\sigma^{f\ mean}_{22}$ the effect of the substrate is very small. Also, we observe that $\sigma^{f\ mean}_{11}$ is larger in magnitude compared to $\sigma^{f\ mean}_{22}$; a reasonable result, since the strain is along the Θ^1 direction.

For the case of $\sigma^{f\ mean}_{12}$ of Fig. 1(c) the effect of the substrate is significant. This is due to the fact that in Eq. (37) there is no term solely from graphene in order to dominate. All terms in this equation contain the substrate's modulus λ, μ. Thus, $\sigma^{f\ mean}_{12}$ is affected significantly from the substrate. Fig. 1(c) has two scales on the y-axis. The left scale measure stress in GPa for the PMMA and the PET substrate, while the right scale measure stress in MPa for the PDMS substrate which is significantly softer than the other two choices. So, for the component $\sigma^{f\ mean}_{12}$ the effect of the substrate is significant. Also, we observe that $\sigma^{f\ mean}_{12}$ is much smaller in magnitude (more than three orders of magnitude) compared to $\sigma^{f\ mean}_{11}$, $\sigma^{f\ mean}_{22}$ and this difference become even more intense with a softer substrate.

In real world it is sometime common to have a field of internal strain for the film or the substrate after the production process. To take this into account into our model, we add in the above analysis a field of in-surface internal strain, $0 \neq e^{0\ bulk}_{11} \neq e^{0\ bulk}_{11} \neq 0$, to obtain for the shift vector components

$$p_1 = \frac{1}{c_9}[-\lambda e^{0\,b}_{11} n^b_1 - 2\mu e^{0\,b}_{11} n^b_1 - \lambda\epsilon_1 n^b_1 - 2\mu\epsilon_1 n^b_1], \tag{38}$$

$$p_2 = \frac{1}{c_9}[-\lambda e^{0\,b}_{11} n^b_2 - \lambda\epsilon_1 n_2 + c_5 e^{0\,f}_{11} + c_5\epsilon_1]. \tag{39}$$

The constitutive law for this case then read

$$\sigma^f_{11} = c_1 e^{0\,f}_{11} + c_1\epsilon_1 - \frac{c_5}{c_9}[-\lambda e^{0\,b}_{11} n^b_2 - \lambda\epsilon_1 n^b_2 + c_5 e^{0\,f}_{11} + c_5\epsilon_1], \tag{40}$$

$$\sigma^f_{22} = c_2 e^{0\,f}_{11} + c_2\epsilon_1 + \frac{c_5}{c_9}[-\lambda e^{0\,b}_{11} n^b_2 - \lambda\epsilon_1 n^b_2 + c_5 e^{0\,f}_{11} + c_5\epsilon_1], \tag{41}$$

$$\sigma^f_{12} = -2\frac{c_5}{c_9}[-\lambda e^{0\,b}_{11} n^b_1 - 2\mu e^{0\,b}_{11} n^b_1 - \lambda\epsilon_1 n^b_1 - 2\mu\epsilon_1 n^b_1]. \tag{42}$$

We define again the mean stress components as

$$\sigma^{f\ mean}_{ij} = \int_0^1 \int_0^1 \sigma^f_{ij}(\Theta^1, \Theta^2) d\Theta^1 d\Theta^2, \tag{43}$$

to obtain

$$\sigma^{f\ mean}_{11} = c_1 e^{0\,f}_{11} + c_1\epsilon_1 - \frac{c_5}{c_9}\left[-\frac{\lambda}{2} e^{0\,b}_{11} - \frac{\lambda}{2}\epsilon_1 + c_5 e^{0\,f}_{11} + c_5\epsilon_1\right], \tag{44}$$

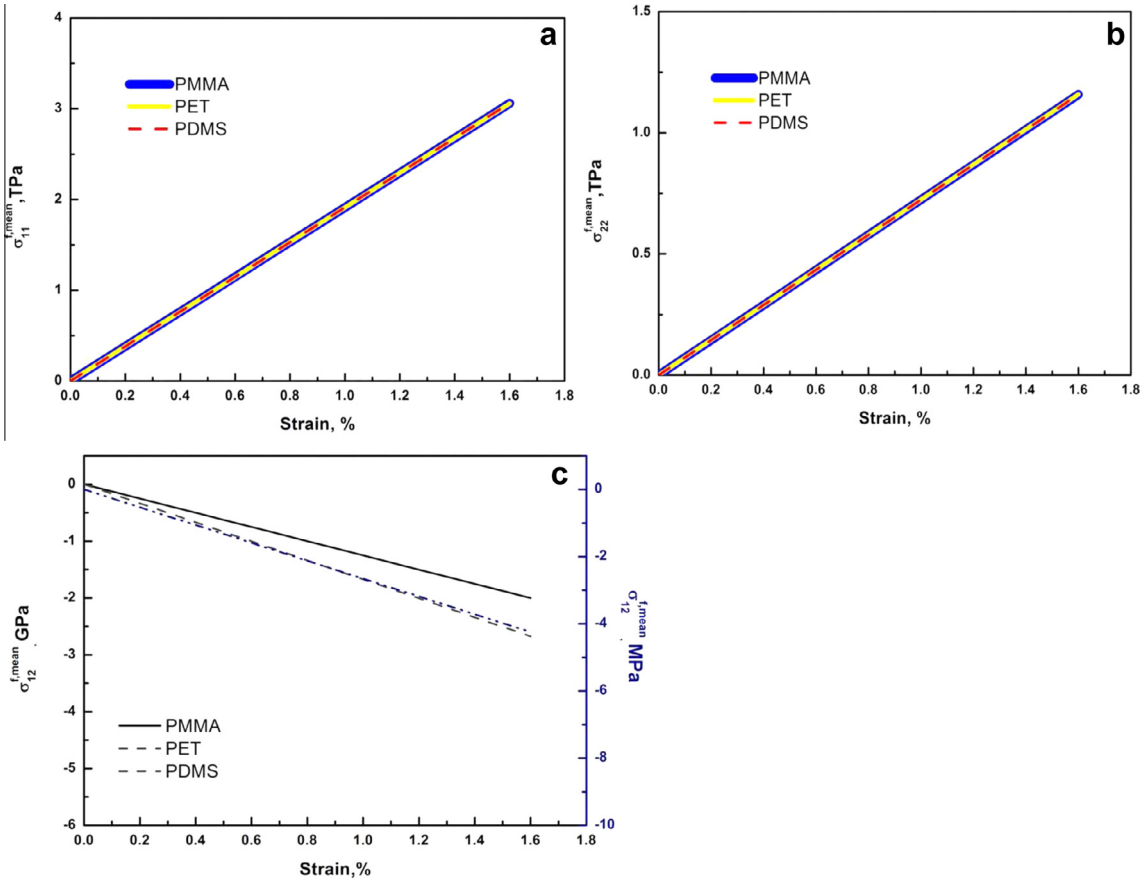

Fig. 1. (a) $\sigma_{11}^{f\ mean}$ versus ϵ_1, (b) $\sigma_{22}^{f\ mean}$ versus ϵ_1, (c) $\sigma_{12}^{f\ mean}$ versus ϵ_1 for the axial strain problem from Eqs. (35)–(37).

$$\sigma_{22}^{f\ mean} = c_2 e_{11}^{0\ f} + c_2\epsilon_1 + \frac{c_5}{c_9}\left[-\frac{\lambda}{2}e_{11}^{0\ b} - \frac{\lambda}{2}\epsilon_1 + c_5 e_{11}^{0\ f} + c_5\epsilon_1\right], \tag{45}$$

$$\sigma_{12}^{f\ mean} = -2\frac{c_5}{c_9}\left[-\frac{\lambda}{2}e_{11}^{0\ b} - 2\frac{\mu}{2}e_{11}^{0\ b} - \frac{\lambda}{2}\epsilon_1 - 2\frac{\mu}{2}\epsilon_1 n_1^b\right]. \tag{46}$$

Fig. 2(a) give $\sigma_{11}^{f\ mean}$ versus ϵ_1 for $e_{11}^{0\ f} = 0.2\%$, $e_{11}^{0\ b} = 0.1\%$. Fig. 2(b) give $\sigma_{22}^{f\ mean}$ versus ϵ_1 while Fig. 2(c) give $\sigma_{12}^{f\ mean}$ versus ϵ_1 for $e_{11}^{0\ f} = 0.2\%$, $e_{11}^{0\ b} = 0.1\%$. These Figures take into account the effect the residual strains has on the $\sigma_{ij}^{f\ mean}$ versus ϵ_1 curves. Strain is again measured through ϵ_1 and we evaluate the curves for $\epsilon_1 = 0 - 1.6\%$. As expected, the presence of the field of internal strains does not alter the form the diagrams have. It shifts them up in the y-axis to describe the residual strain field. So all comments concerning Fig. 1 are valid here as well with the only difference that the curve does not meet the origin of the axis. Since this effect is very small, within each Fig. 2(a)–(c) we make a smaller plot where we magnify the neighborhood of $(0, 0)$. This smaller figure highlight the effect of the residual strains in the neighborhood of the origin of the axis.

3.2. Simple shear

We introduce simple shear by assuming for the displacement components (Sfyris et al., 2014a,b) ($\mathbf{u}^b = \mathbf{u}^f = \mathbf{u}$)

$$u_1 = \Theta^1 + \epsilon\Theta^2, \quad u_2 = \Theta^2. \tag{47}$$

The first equation ruling the shift vector can then be solved to give

$$p_1 = \frac{1}{c_9}\left[-\lambda(e_{11}^{0\ b} + e_{22}^{0\ b})n_1^b - 2\mu e_{11}^{0\ b}n_1^b - 2\mu e_{12}^{0\ b}n_2^b - c_9 p_1^0 + 2c_5 e_{12}^{0\ f} - \mu\epsilon n_2^b + c_5\epsilon\right]. \tag{48}$$

The second equation ruling the shift vector finally lead at

$$p_2 = \frac{1}{c_9}\left[-\lambda(e_{11}^{0\ b} + e_{22}^{0\ b})n_2^b - 2\mu e_{21}^{0\ b}n_1^b - 2\mu e_{22}^{0\ b}n_2^b - \mu\epsilon n_1^b - c_9 p_2^0 + c_5 e_{11}^{0\ f} + c_5 e_{22}^{0\ f}\right]. \tag{49}$$

The first equation of momentum then read

$$\begin{aligned}&\lambda(e_{11}^{0\ b} + e_{22}^{0\ b} + e_{33}^{0\ b})n_1^b + 2\mu e_{11}^{0\ b}n_1^b + 2\mu e_{12}^{0\ b}n_2^b + 2\mu e_{13}^{0\ b}n_3^b + \mu\epsilon n_2^b \\ &+ c_1 e_{11,1}^{0\ f} + c_2 e_{22,1}^{0\ f} + c_3 b_{11,1}^{0\ f} + c_4 b_{22,1}^{0\ f} - c_5 p_{2,1}^0 + \frac{c_1 - c_2}{2}e_{12,2}^{0\ f} \\ &+ \frac{c_3 - c_4}{2}b_{12,2}^{0\ f} - 2c_5 p_{1,2}^0 + -\frac{c_5}{c_9}\left[-\lambda(e_{11}^{0\ b} + e_{22}^{0\ b})n_2^b\right. \\ &\left.-2\mu e_{21}^{0\ b}n_1^b - 2\mu e_{22}^{0\ b}n_2^b - \mu\epsilon n_1^b - c_9 p_2^0 + c_5 e_{11}^{0\ f} + c_5 e_{22}^{0\ f}\right]_{,1} \\ &-2\frac{c_5}{c_9}\left[-\lambda(e_{11}^{0\ b} + e_{22}^{0\ b})n_1^b - 2\mu e_{11}^{0\ b}n_1^b - 2\mu e_{12}^{0\ b}n_2^b - c_9 p_1^0\right. \\ &\left.+2c_5 e_{12}^{0\ f} - \mu\epsilon n_2^b + c_5\epsilon\right]_{,2} = 0.\end{aligned} \tag{50}$$

For the second equation of momentum we take

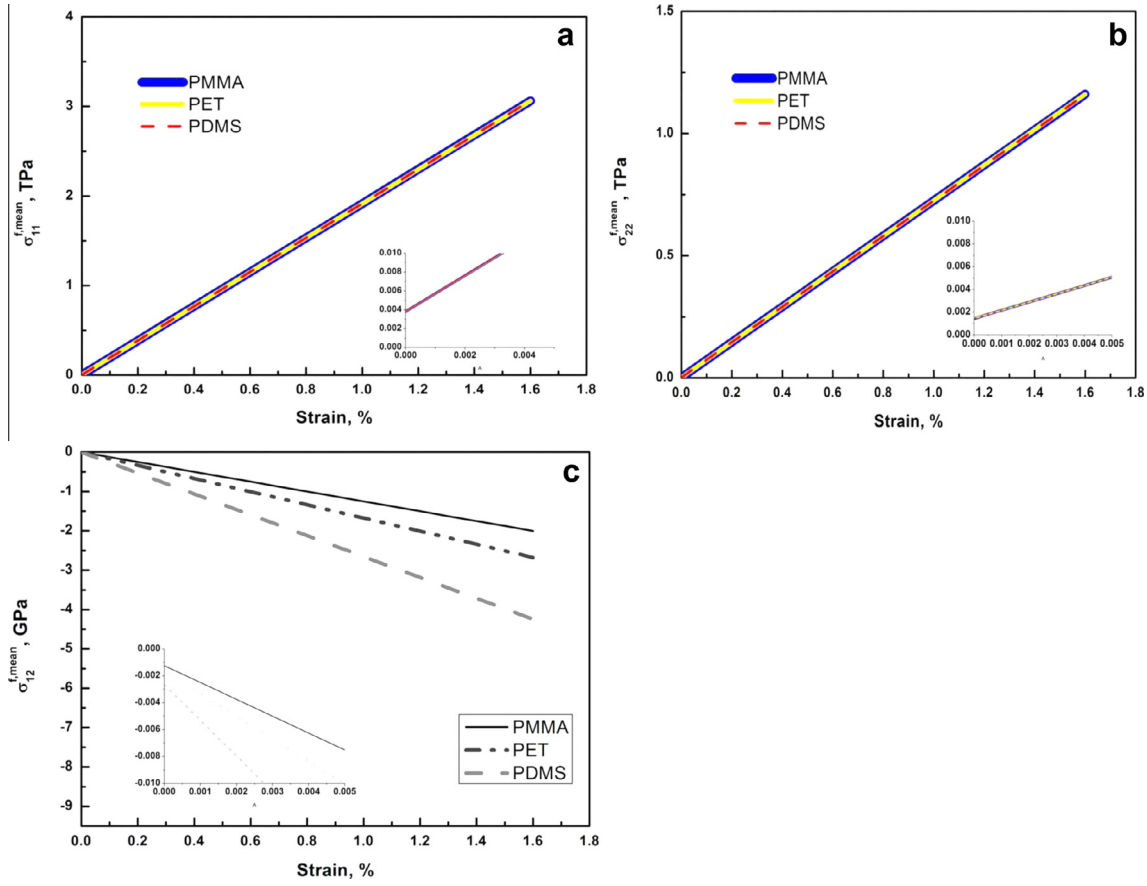

Fig. 2. $\sigma_{11}^{f\ mean}$ versus ϵ_1, (b) $\sigma_{22}^{f\ mean}$ versus ϵ_1, (c) $\sigma_{12}^{f\ mean}$ versus ϵ_1 for the axial strain problem with internal strains, $e_{11}^{0\ f}=0.2\%$, $e_{11}^{0\ b}=0.1\%$, from Eqs. (44)–(46).

$$\lambda(e_{11}^{0\ b}+e_{22}^{0\ b}+e_{33}^{0\ b})n_2^b+2\mu e_{21}^{0\ b}n_1^b+2\mu e_{22}^{0\ b}n_2^b+2\mu e_{23}^{0\ b}n_3^b+\mu\epsilon n_1^b$$
$$+c_2e_{11,2}^{0\ f}+c_1e_{22,2}^{0\ f}+c_4b_{11,2}^{0\ f}+c_3b_{22,2}^{0\ f}+c_5p_{2,2}^0+\frac{c_1-c_2}{2}e_{12,1}^{0\ f}$$
$$+\frac{c_3-c_4}{2}b_{12,1}^{0\ f}-2c_5p_{1,1}^0+-2\frac{c_5}{c_9}\left[-\lambda(e_{11}^{0\ b}+e_{22}^{0\ b})n_1^b-2\mu e_{11}^{0\ b}n_1^b\right.$$
$$\left.-2\mu e_{12}^{0\ b}n_2^b-c_9p_1^0+2c_5e_{12}^{0\ f}-\mu\epsilon n_2^b+c_5\epsilon\right]_{,1}$$
$$+\frac{c_5}{c_9}\left[-\lambda(e_{11}^{0\ b}+e_{22}^{0\ b})n_2^b-2\mu e_{21}^{0\ b}n_1^b-2\mu e_{22}^{0\ b}n_2^b-\mu\epsilon n_1^b-c_9p_2^0\right.$$
$$\left.+c_5e_{11}^{0\ f}+c_5e_{22}^{0\ f}\right]_{,2}=0. \tag{51}$$

The equations of momentum, Eqs. (50) and (51), render conditions that the field of internal strains, the strain constant, ϵ, the vector $\mathbf{n}^b$ and the material parameters, c_1, c_2, c_5, c_9, λ, μ, should satisfy in order Eq. (47) to be a solution for all field equations.

The constitutive law for the stresses are then

$$\sigma_{11}^f=c_1e_{11}^{0\ f}+c_2e_{22}^{0\ f}-c_5p_2^0-\frac{c_5}{c_9}[-\lambda(e_{11}^{0\ b}+e_{22}^{0\ b})n_2^b$$
$$-2\mu e_{21}^{0\ b}n_1^b-2\mu e_{22}^{0\ b}n_2^b-\mu\epsilon n_1^b-c_9p_2^0+c_5e_{11}^{0\ f}$$
$$+c_5e_{22}^{0\ f}], \tag{52}$$

$$\sigma_{22}^f=c_2e_{11}^{0\ f}+c_1e_{22}^{0\ f}+c_5p_2^0+\frac{c_5}{c_9}[-\lambda(e_{11}^{0\ b}+e_{22}^{0\ b})n_2^b$$
$$-2\mu e_{21}^{0\ b}n_1^b-2\mu e_{22}^{0\ b}n_2^b-\mu\epsilon n_1^b-c_9p_2^0+c_5e_{11}^{0\ f}$$
$$+c_5e_{22}^{0\ f}], \tag{53}$$

$$\sigma_{12}^f=\frac{c_1-c_2}{2}e_{12}^{0\ f}-2c_5p_1^0+\frac{c_1-c_2}{4}\epsilon-2\frac{c_5}{c_9}[-\lambda(e_{11}^{0\ b}+e_{22}^{0\ b})n_1^b$$
$$-2\mu e_{11}^{0\ b}n_1^b-2\mu e_{12}^{0\ b}n_2^b-c_9p_1^0+2c_5e_{12}^{0\ f}-\mu\epsilon n_2^b+c_5\epsilon]. \tag{54}$$

The particular case when there are no internal strains render for the shift vector components

$$p_1=\frac{1}{c_9}[-\mu\epsilon n_2^b+c_5\epsilon], \tag{55}$$

$$p_2=\frac{1}{c_9}[-\mu\epsilon n_1^b]. \tag{56}$$

For the stress components we then have

$$\sigma_{11}^f=-\frac{c_5}{c_9}[-\mu\epsilon n_1^b], \tag{57}$$

$$\sigma_{22}^f=+\frac{c_5}{c_9}[-\mu\epsilon n_1^b], \tag{58}$$

$$\sigma_{12}^f=\frac{c_1-c_2}{4}\epsilon-2\frac{c_5}{c_9}[-\mu\epsilon n_2^b+c_5\epsilon]. \tag{59}$$

If we introduce the mean stress components as in the previous subsection we finally take

$$\sigma_{11}^{f\ mean}=-\frac{c_5}{c_9}\left[-\frac{\mu}{2}\epsilon\right], \tag{60}$$

$$\sigma_{22}^{f\ mean}=+\frac{c_5}{c_9}\left[-\frac{\mu}{2}\epsilon\right], \tag{61}$$

$$\sigma_{12}^{f\ mean}=\frac{c_1-c_2}{4}\epsilon-2\frac{c_5}{c_9}\left[-\frac{\mu}{2}\epsilon+c_5\epsilon\right]. \tag{62}$$

Fig. 3 give the mean stress versus strain curves evaluated from Eqs. (60)–(62). Strain here is measured through ϵ, for which we assume $\epsilon=0-1.6\%$. Fig. 3(a) plot $\sigma_{11}^{f\ mean}$ versus ϵ, Fig. 3(b) plot

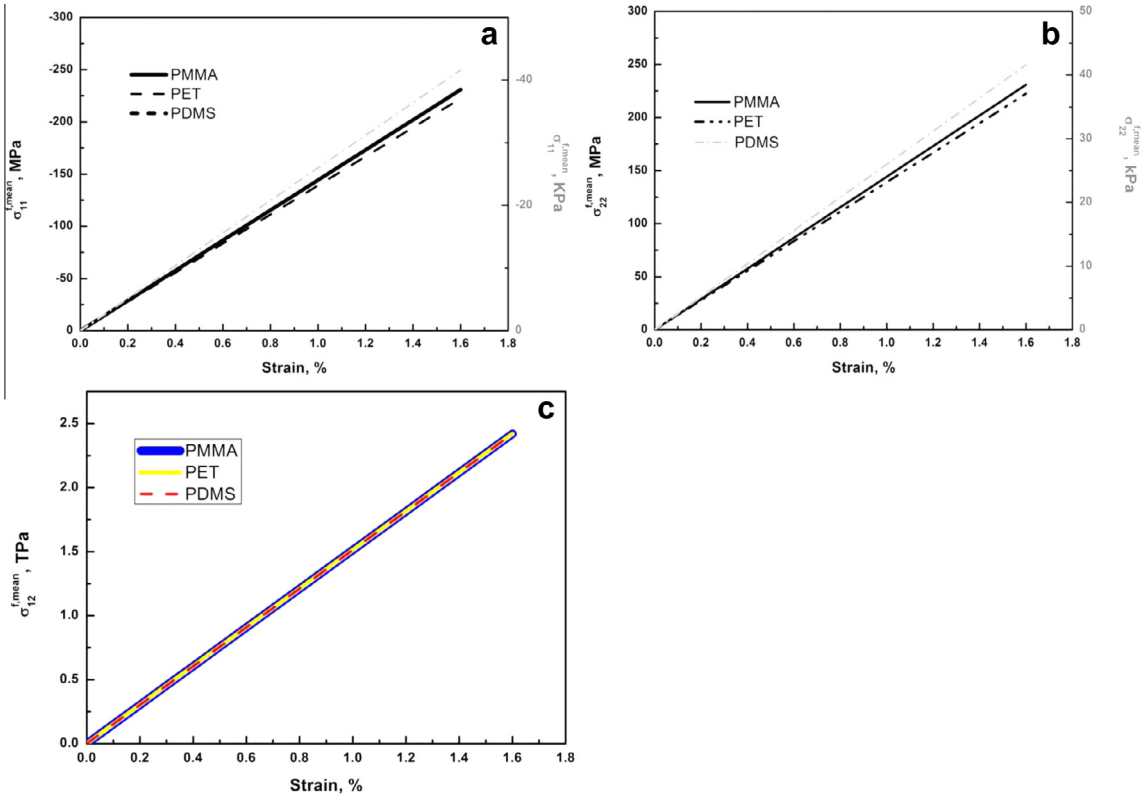

Fig. 3. $\sigma_{11}^{f\ mean}$ versus ϵ, (b) $\sigma_{22}^{f\ mean}$ versus ϵ, (c) $\sigma_{12}^{f\ mean}$ versus ϵ for the simple shear problem from Eqs. (60)–(62).

$\sigma_{22}^{f\ mean}$ versus ϵ, while Fig. 3(c) plot $\sigma_{12}^{f\ mean}$ versus ϵ. From Eqs. (60) and (61) we see that the effect of the substrate is significant for $\sigma_{11}^{f\ mean}$, $\sigma_{22}^{f\ mean}$ since the Lame constant μ of the substrate is present in both of them. Fig. 3(a) and (b) have two scales: on the left scale the units are MPa, while on the right scale they are kPa. The MPA measurements pertain to the PMMA and the PET substrate, while the kPa scale pertain to the PDMS measurement. Thus, for the simple shear strain problem $\sigma_{11}^{f\ mean}$, $\sigma_{22}^{f\ mean}$ are affected significantly from the presence of the substrate. The softer the substrate is, the smaller the components $\sigma_{11}^{f\ mean}$, $\sigma_{22}^{f\ mean}$ are.

On the other hand the effect of the substrate on the $\sigma_{12}^{f\ mean}$ component is insignificant. This is seen in Fig. 3(c), where all curves are almost equivalent. This is reasonable if one inspect Eq. (62). In this equation, the first and the third term come solely from the film so they are the dominant terms and the effect of the substrate is very small. We also observe that $\sigma_{12}^{f\ mean}$ is larger in magnitude (more than three orders of magnitude) from $\sigma_{11}^{f\ mean}$, $\sigma_{22}^{f\ mean}$ and this difference become more intense with softer substrate. This is reasonable since the only non-trivial component corresponding to Eq. (47) is the e_{12}^{f} component.

When there is a field of internal strain for the film, $e_{12}^{0\,f}$, as well as for the bulk, $e_{12}^{0\,b}$, for the shift vector components we obtain

$$p_1 = \frac{1}{c_9}[-2\mu e_{12}^{0\,b} n_2^b + 2c_5 e_{12}^{0\,f} - \mu\epsilon n_2^b + c_5\epsilon], \tag{63}$$

$$p_2 = \frac{1}{c_9}[-2\mu e_{12}^{0\,b} n_1^b - \mu\epsilon n_1^b]. \tag{64}$$

For the stress vector components we then have

$$\sigma_{11}^{f} = -\frac{c_5}{c_9}[-2\mu e_{12}^{0\,b} n_1^b - \mu\epsilon n_1^b]. \tag{65}$$

$$\sigma_{22}^{f} = +\frac{c_5}{c_9}[-2\mu e_{12}^{0\,b} n_1^b - \mu\epsilon n_1^b]. \tag{66}$$

$$\sigma_{12}^{f} = \frac{c_1 - c_2}{2} e_{12}^{0\,f} + \frac{c_1 - c_2}{4}\epsilon - 2\frac{c_5}{c_9}[-2\mu e_{12}^{0\,b} n_2^b + 2c_5 e_{12}^{0\,f} - \mu\epsilon n_2^b + c_5\epsilon]. \tag{67}$$

Then the mean stress components are

$$\sigma_{11}^{f\ mean} = -\frac{c_5}{c_9}\left[-\mu e_{12}^{0\,b} - \frac{\mu}{2}\epsilon\right]. \tag{68}$$

$$\sigma_{22}^{f\ mean} = +\frac{c_5}{c_9}\left[-\mu e_{12}^{0\,b} - \frac{\mu}{2}\epsilon\right]. \tag{69}$$

$$\sigma_{12}^{f\ mean} = \frac{c_1 - c_2}{2} e_{12}^{0\,f} + \frac{c_1 - c_2}{4}\epsilon - 2 \times \frac{c_5}{c_9}\left[-\mu e_{12}^{0\,b} + 2c_5 e_{12}^{0\,f} - \frac{\mu}{2}\epsilon + c_5\epsilon\right]. \tag{70}$$

Fig. 4(a) give $\sigma_{11}^{f\ mean}$ versus ϵ for $e_{12}^{0\,f} = 0.2\%$, $e_{12}^{0\,b} = 0.1\%$. Fig. 4(b) give $\sigma_{22}^{f\ mean}$ versus ϵ while Fig. 4(c) give $\sigma_{12}^{f\ mean}$ versus ϵ for $e_{12}^{0\,f} = 0.2\%$, $e_{12}^{0\,b} = 0.1\%$. These figures take into account the effect the residual strains has on the $\sigma_{ij}^{f\ mean}$ versus ϵ curves. Strain is again measured through ϵ and we evaluate the curves for $\epsilon = 0 - 1.6\%$. As expected, the presence of the field of internal strains does not alter the form the diagrams have. It shifts them up in the y-axis to describe the residual strain field. So all comments concerning Fig. 4 are valid here as well with the only difference that the curve does not meet the origin of the axis. Since this effect is very small, within each Fig. 4(a)–(c) we make a smaller plot where we magnify the neighborhood of $(0, 0)$. This smaller figure highlight the effect of the residual strains in the neighborhood of the origin of the axis.

Please cite this article in press as: Sfyris, D., et al. Graphene resting on substrate: Closed form solutions for the perfect bonding and the delamination case. Int. J. Solids Struct. (2015), http://dx.doi.org/10.1016/j.ijsolstr.2015.06.024

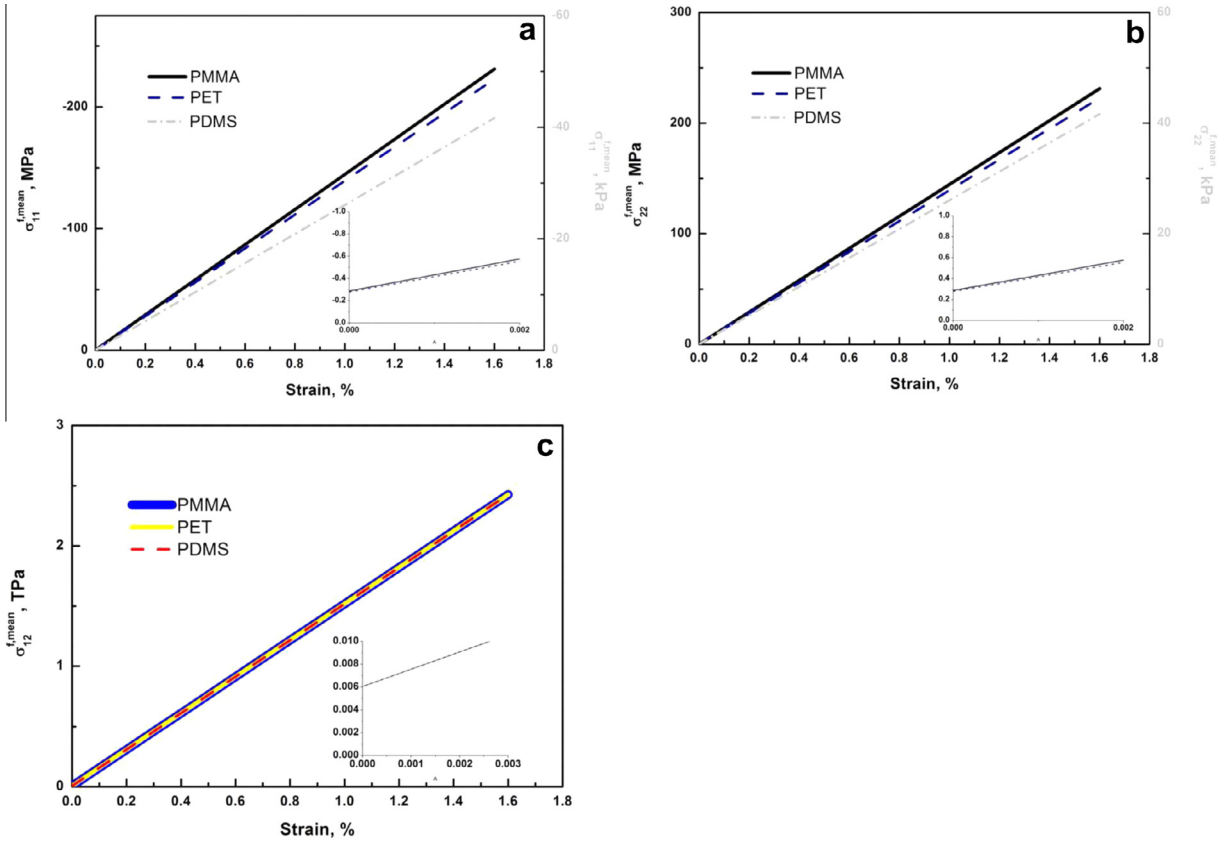

Fig. 4. $\sigma_{11}^{f\ mean}$ versus ϵ, (b) $\sigma_{22}^{f\ mean}$ versus ϵ, (c) $\sigma_{12}^{f\ mean}$ versus ϵ for the simple shear problem with internal strains, $e_{12}^{0\,f} = 0.2\%, e_{12}^{0\,b} = 0.1\%$, from Eqs. (68)–(70).

4. Out-of-surface motions-perfect bonding

We here follow our previous approach (Sfyris et al., 2014a,b) and model tension/compression that ultimately leads to buckling by assuming for the displacement the form

$$\mathbf{u}(\Theta^1,\Theta^2) = \left(\epsilon\Theta^1, \Theta^2, \cos\left(\frac{n\pi\Theta^1}{2L_1}\right) f(\Theta^2)\right). \tag{71}$$

These would be the components of the displacement field for both the film and the substrate since we still assume perfect bonding. We should, however, note that while for the substrate out-of-surface motions are introduced through the term n_3^b, for the film they are described by the terms of the curvature tensor, $\mathbf{b}^f$.

For our framework, $\mathbf{b}^f$ is the second fundamental form of the surface, so we evaluate for its components (Sfyris et al., 2014a,b)

$$b_{11}^f = -\epsilon\frac{n^2\pi^2}{4L_1^2}\cos\left(\frac{n\pi\Theta^1}{2L_1}\right) f(\Theta^2), \tag{72}$$

$$b_{12}^f = b_{21} = -\epsilon\frac{n\pi}{2L_1}\cos\left(\frac{n\pi\Theta^1}{2L_1}\right) f'(\Theta^2), \tag{73}$$

$$b_{22}^f = \epsilon\cos\left(\frac{n\pi\Theta^1}{2L_1}\right) f(\Theta^2). \tag{74}$$

The outward unit normal, $\mathbf{n}^b$, is then defined by

$$\mathbf{n}^b = \frac{\mathbf{u}_{,1}\times\mathbf{u}_{,2}}{|\mathbf{u}_{,1}\times\mathbf{u}_{,2}|}. \tag{75}$$

So, for the surface described by Eq. (71) the outward unit normal has componential form

$$\mathbf{n}^b = \left(-\frac{n\pi}{2L_1}\sin\left(\frac{n\pi\Theta^1}{2L_1}\right) f(\Theta^2), -\epsilon\cos\left(\frac{n\pi\Theta^1}{2L_1}\right) f'(\Theta^2), \epsilon\right), \tag{76}$$

when for its Euclidean length we assume it is unity:

$$\|\mathbf{n}^b\| = \sqrt{\left[-\frac{n\pi}{2L_1}\sin\left(\frac{n\pi\Theta^1}{2L_1}\right) f(\Theta^2)\right]^2 + \left[-\epsilon\cos\left(\frac{n\pi\Theta^1}{2L_1}\right) f'(\Theta^2)\right]^2 + \epsilon^2} = 1. \tag{77}$$

We evaluate the necessary derivatives as

$$u_{1,1} = \epsilon, \quad u_{1,2} = 0 = u_{2,1}, \quad u_{2,2} = 0, \tag{78}$$

$$u_{3,1} = -\frac{n\pi}{2L_1} sin\left(\frac{n\pi\Theta^1}{2L_1}\right) f(\Theta^2), \tag{79}$$

$$u_{3,2} = cos\left(\frac{n\pi\Theta^1}{2L_1}\right) f'(\Theta^2). \tag{80}$$

So, the first equation for the shift vector, Eq. (19), render

$$p_1 = \frac{1}{c_9}[-\lambda(e_{11}^{0\,b} + e_{22}^{0\,b} + e_{33}^{0\,b})n_1^b - 2\mu e_{11}^{0\,b} n_1^b - 2\mu e_{12}^{0\,b} n_2^b - 2\mu e_{13}^{0\,b} n_3^b - \lambda\epsilon n_1^b - c_9 p_1^0 + 2c_5 e_{12}^{0\,f} + 2c_8 b_{12}^{0\,f} - \mu u_{3,1}^b n_3^b + 2c_8 b_{12}^f]. \tag{81}$$

The second equation for the shift vector, Eq. (20), give

$$p_1 = \frac{1}{c_9}[-\lambda(e_{11}^{0\,b} + e_{22}^{0\,b} + e_{33}^{0\,b})n_2^b - 2\mu e_{21}^{0\,b} n_1^b - 2\mu e_{22}^{0\,b} n_2^b - 2\mu e_{23}^{0\,b} n_3^b - \lambda\epsilon n_2^b - c_9 p_2^0 + c_5 e_{11}^{0\,f} + c_5 e_{22}^{0\,f} - c_8 b_{11}^{0\,f} - c_8 b_{22}^{0\,f} - \mu u_{3,2}^b n_3^b + c_5\epsilon + c_8 b_{11}^f - c_8 b_{22}^f]. \tag{82}$$

Substituting these expressions to the first of the momentum equation, Eq. (17), we obtain after some caclulations

$$A(\Theta^1,\Theta^2)f''(\Theta^2)+B(\Theta^1,\Theta^2)f'(\Theta^2)+C(\Theta^1,\Theta^2)f(\Theta^2)+D(\Theta^1,\Theta^2)=0. \tag{83}$$

For terms A, B, C, D we have

$$A(\Theta^1,\Theta^2)=\left[-4\epsilon\frac{c_5}{c_9}\mu e_{12}^{0\ b}-\frac{c_3-c_4}{2}\epsilon+5\frac{c_5c_8}{c_9}\epsilon-\epsilon c_4\right]\frac{n\pi}{2L_1}\times\sin\left(\frac{n\pi\Theta^1}{2L_1}\right), \tag{84}$$

$$\begin{aligned}B(\Theta^1,\Theta^2)=&\left[-2\mu e_{12}^{0\ b}+\frac{c_5}{c_9}[-\lambda(e_{11,1}^{0\ b}+e_{22,1}^{0\ b}+e_{33,1}^{0\ b})-2\mu e_{22,1}^{0\ b}]\right]\times\cos\left(\frac{n\pi\Theta^1}{2L_1}\right)-\left[\frac{c_5}{c_9}[-\lambda(e_{11}^{0\ b}+e_{22}^{0\ b}+e_{33}^{0\ b})-2\mu e_{22}^{0\ b}\right.\\&\left.-\lambda\epsilon+3\mu\epsilon]\right]\frac{n\pi}{2L_1}\sin\left(\frac{n\pi\Theta^1}{2L_1}\right)+\left[2\frac{c_5}{c_9}[-\lambda(e_{11}^{0\ b}+e_{22}^{0\ b}+e_{33}^{0\ b})-2\mu e_{11}^{0\ b}-\lambda\epsilon]\right]\frac{n\pi}{2L_1}\\&\times\sin\left(\frac{n\pi\Theta^1}{2L_1}\right),\end{aligned} \tag{85}$$

$$\begin{aligned}C(\Theta^1,\Theta^2)=&-\left[2\frac{c_5}{c_9}[-\lambda(e_{11,2}^{0\ b}+e_{22,2}^{0\ b}+e_{33,2}^{0\ b})-2\mu e_{11,2}^{0\ b}]\right]\frac{n\pi}{2L_1}\times\sin\left(\frac{n\pi\Theta^1}{2L_1}\right)\left[-\mu\epsilon-\frac{c_5c_8\epsilon}{c_9}\frac{n^2\pi^2}{4L_1^2}+c_3\epsilon\frac{n^2\pi^2}{4L_1^2}\right]\frac{n\pi}{2L_1}\\&\times\sin\left(\frac{n\pi\Theta^1}{2L_1}\right)-[\lambda(e_{11}^{0\ b}+e_{22}^{0\ b}+e_{33}^{0\ b})+2\mu e_{11}^{0\ b}+\lambda\epsilon+2\mu]\frac{n\pi}{2L_1}\cos\left(\frac{n\pi\Theta^1}{2L_1}\right),\\&-\left[-2\mu e_{22,1}^{0\ b}-2\mu\frac{c_5}{c_8}e_{21}^{0\ b}\frac{n\pi}{2L_1}\right]\frac{n\pi}{2L_1}\cos\left(\frac{n\pi\Theta^1}{2L_1}\right),\end{aligned} \tag{86}$$

$$\begin{aligned}D(\Theta^1,\Theta^2)=&\,2\mu e_{13}^{0\ b}\epsilon+c_1e_{11,1}^{0\ f}-c_2e_{22,1}^{0\ f}+c_3b_{11,1}^{0\ f}+c_4b_{22,1}^{0\ f}-c_5p_{2,1}^0+\frac{c_1-c_2}{2}e_{12,1}^{0\ f}+\frac{c_3-c_4}{2}b_{12,1}^{0\ f}-2c_5p_{1,2}^0\\&-\frac{c_5}{c_9}[-2\mu\epsilon e_{23,1}^{0\ b}-c_9p_{2,1}^0+c_5e_{11,1}^{0\ f}+c_5e_{22,1}^{0\ f}-c_8b_{11,1}^{0\ f}-c_8b_{22,1}^{0\ f}]-2\frac{c_5}{c_9}[-2\mu\epsilon e_{13,2}^{0\ b}-c_9p_{1,2}^0\\&+2c_5e_{12,2}^{0\ f}+2c_8b_{12,2}^{0\ f}].\end{aligned} \tag{87}$$

To proceed we follow an analysis used elsewhere (Sfyris et al., 2008) and we consider the particular case where there exist a function $\Psi=\Psi(\Theta^1,\Theta^2)$ such that

$$A(\Theta^1,\Theta^2)=\alpha\Psi(\Theta^1,\Theta^2), \tag{88}$$

$$B(\Theta^1,\Theta^2)=\beta\Psi(\Theta^1,\Theta^2), \tag{89}$$

$$C(\Theta^1,\Theta^2)=\gamma\Psi(\Theta^1,\Theta^2), \tag{90}$$

$$D(\Theta^1,\Theta^2)=\delta\Psi(\Theta^1,\Theta^2). \tag{91}$$

In this case Eq. (83) for the function f read

$$\alpha f''(\Theta^2)+\beta f'(\Theta^2)+\gamma f(\Theta^2)+\delta=0, \tag{92}$$

while the existence of the function Ψ equals to

$$\frac{A(\Theta^1,\Theta^2)}{\alpha}=\frac{B(\Theta^1,\Theta^2)}{\beta}=\frac{C(\Theta^1,\Theta^2)}{\gamma}=\frac{D(\Theta^1,\Theta^2)}{\delta}. \tag{93}$$

We split Eq. (92) into its inhomogeneous and homogeneous part. The homogeneous part can be solved by the technique of the characteristic polynomial to give the solutions

$$c_{11}e^{\lambda_1\Theta^2}+c_{22}e^{\lambda_2\Theta^2}, \tag{94}$$

$c_{11},\ c_{22}$, being constants. The characteristic polynomial has two distinct roots

$$\lambda_{1,2}=\frac{-\beta\pm\sqrt{\beta^2-4\alpha\gamma}}{2\alpha}. \tag{95}$$

In this case, the function $f(\Theta^2)$ that solves Eq. (92) is given as

$$f(\Theta^2)=c_{11}e^{\lambda_1\Theta^2}+c_{22}e^{\lambda_2\Theta^2}-\frac{\delta}{\gamma}, \tag{96}$$

since $\frac{\delta}{\gamma}$ is a particular solution of Eq. (92). Constants $\alpha,\ \beta,\ \gamma,\ \delta$ should satisfy Eq. (93). All in all, Eq. (71) qualifies as a solution when f is given by Eq. (96) and the loading constant ϵ, graphene's material moduli $c_i,\ i=1,\dots,9$, substrate's moduli λ,μ and internal strains satisfy Eq. (93). Additionally, the second component of the momentum equation should be satisfied as well as the moment of momentum equations. We refrain from writing them, due to its being lengthy, but we stress that one can compute them straightforwardly.

When there is a double eigenvalue $\lambda_{1,2}=\frac{-\beta}{2\alpha}$ the function f should be substituted by the expression

$$f(\Theta^2)=c_{11}e^{\lambda\Theta^2}+c_{22}\Theta^2e^{\lambda\Theta^2}-\frac{\delta}{\gamma}. \tag{97}$$

To particularize our approach we assume that $\beta=2,\ \alpha=\gamma=\delta=1$, so we have one double root $\lambda_{1,2}=-1$. The function f in this case read

$$f(\Theta^2)=e^{-\Theta^2}+\Theta^2e^{-\Theta^2}-1, \tag{98}$$

so for the displacement field we have

$$\mathbf{u}(\Theta^1,\Theta^2)=\left(\epsilon\Theta^1,\Theta^2,\cos\left(\frac{n\pi\Theta^1}{2L_1}\right)(e^{-\Theta^2}+\Theta^2e^{-\Theta^2}-1)\right). \tag{99}$$

The components for the shift vector are then

$$p_1=\frac{1}{c_9}[\lambda+\mu]\epsilon\frac{n\pi}{2L_1}\sin\left(\frac{n\pi\Theta^1}{2L_1}\right)(e^{-\Theta^2}+\Theta^2e^{-\Theta^2}-1)+2\frac{c_8}{c_9}\epsilon\frac{n\pi}{2L_1}\sin\left(\frac{n\pi\Theta^1}{2L_1}\right)\Theta^2e^{-\Theta^2}, \tag{100}$$

$$\begin{aligned}p_2=&\frac{1}{c_9}[c_5\epsilon+(\mu-\lambda\epsilon)\epsilon\cos\left(\frac{n\pi\Theta^1}{2L_1}\right)\Theta^2e^{-\Theta^2}]-c_8\epsilon\frac{n^2\pi^2}{4L_1^2}\times\cos\left(\frac{n\pi\Theta^1}{2L_1}\right)(e^{-\Theta^2}+\Theta^2e^{-\Theta^2}-1)\\&-c_8\epsilon\cos\left(\frac{n\pi\Theta^1}{2L_1}\right)(-e^{-\Theta^2}+\Theta^2e^{-\Theta^2})].\end{aligned} \tag{101}$$

For the stress components we evaluate

$$\begin{aligned}\sigma_{11}^f=&\,c_1\epsilon-\frac{c_5^2}{c_9}\epsilon-\left(c_3+\frac{c_5c_8}{c_9}\right)\frac{n^2\pi^2}{4L_1^2}\cos\left(\frac{n\pi\Theta^1}{2L_1}\right)\times(e^{-\Theta^2}+\Theta^2e^{-\Theta^2}-1)+c_4\epsilon\frac{n\pi}{2L_1}\sin\left(\frac{n\pi\Theta^1}{2L_1}\right)\Theta^2e^{-\Theta^2}\\&-\frac{c_5}{c_9}[-\lambda\epsilon+\mu]\epsilon\cos\left(\frac{n\pi\Theta^1}{2L_1}\right)\Theta^2e^{-\Theta^2},\end{aligned} \tag{102}$$

Please cite this article in press as: Sfyris, D., et al. Graphene resting on substrate: Closed form solutions for the perfect bonding and the delamination case. Int. J. Solids Struct. (2015), http://dx.doi.org/10.1016/j.ijsolstr.2015.06.024

$$\sigma_{22}^f = c_2\epsilon + \frac{c_5^2}{c_9}\epsilon - \left[c_4\epsilon + \frac{c_5c_8}{c_9}\epsilon\right]\frac{n^2\pi^2}{4L_1^2}\cos\left(\frac{n\pi\Theta^1}{2L_1}\right) \times (e^{-\Theta^2} + \Theta^2 e^{-\Theta^2} - 1) + c_3\epsilon\frac{n\pi}{2L_1}\sin\left(\frac{n\pi\Theta^1}{2L_1}\right)\Theta^2 e^{-\Theta^2} + \frac{c_5}{c_9}[-\lambda\epsilon^2 + \mu\epsilon]\cos\left(\frac{n\pi\Theta^1}{2L_1}\right)\Theta^2 e^{-\Theta^2}, \quad (103)$$

$$\sigma_{12}^f = [\frac{c_3 - c_4}{2} - 4\frac{c_5c_8}{c_9}]\epsilon\frac{n\pi}{2L_1}\sin\left(\frac{n\pi\Theta^1}{2L_1}\right)\Theta^2 e^{-\Theta^2} - 2\frac{c_5}{c_9}(\lambda+\mu)\epsilon\sin\left(\frac{n\pi\Theta^1}{2L_1}\right)(e^{-\Theta^2} + \Theta^2 e^{-\Theta^2} - 1). \quad (104)$$

For the couple stress components we find

$$m_{11} = c_3\epsilon - \frac{c_8c_5}{c_9}\epsilon - \left(c_6 + \frac{c_8^2}{c_9}\right)\epsilon\frac{n^2\pi^2}{4L_1^2}\cos\left(\frac{n\pi\Theta^1}{2L_1}\right) \times (e^{-\Theta^2} + \Theta^2 e^{-\Theta^2} - 1) + \left(c_7 - \frac{c_8^2}{c_9}\right)\epsilon\cos\left(\frac{n\pi\Theta^1}{2L_1}\right) \times (-e^{-\Theta^2} + \Theta^2 e^{-\Theta^2}) - \frac{c_8}{c_9}(-\lambda\epsilon^2 + \mu\epsilon)\cos\left(\frac{n\pi\Theta^1}{2L_1}\right)\Theta^2 e^{-\Theta^2}, \quad (105)$$

$$m_{22} = c_4\epsilon + \frac{c_8c_5}{c_9}\epsilon - (c_7 + c_8)\epsilon\frac{n^2\pi^2}{4L_1^2}\cos\left(\frac{n\pi\Theta^1}{2L_1}\right) \times (e^{-\Theta^2} + \Theta^2 e^{-\Theta^2} - 1) + \left(c_6 - \frac{c_8^2}{c_9}\right)\cos\left(\frac{n\pi\Theta^1}{2L_1}\right) \times (-e^{-\Theta^2} + \Theta^2 e^{-\Theta^2}) + \frac{c_8}{c_9}(-\lambda\epsilon^2 + \mu\epsilon)\cos\left(\frac{n\pi\Theta^1}{2L_1}\right)\Theta^2 e^{-\Theta^2}, \quad (106)$$

$$m_{12} = \left(\frac{c_6 - c_7}{2} - 4\frac{c_8^2}{c_9}\right)\epsilon\frac{n\pi}{2L_1}\sin\left(\frac{n\pi\Theta^1}{2L_1}\right)\Theta^2 e^{-\Theta^2} \times -2\frac{c_8}{c_9}(\lambda+\mu)\epsilon\frac{n\pi}{2L_1}\sin\left(\frac{n\pi\Theta^1}{2L_1}\right)(e^{-\Theta^2} + \Theta^2 e^{-\Theta^2} - 1). \quad (107)$$

5. Delamination

Distinguishing between $\mathbf{u}^f$ and $\mathbf{u}^b$ in some parts of their common boundary, enables the treatment of delamination. Motivated by the work of Bedrossian and Kohn (2015) we assume for the out-of-surface component of the displacement of the film

$$u_3^f = \begin{cases} \frac{L_1-\phi}{4\pi}\sin\left(\frac{4\pi\Theta^1}{L_1-\phi}\right)g(\Theta^2), & L_1 \leqslant \Theta^1 \leqslant L_1-\phi, L_2 \leqslant \Theta^2 \leqslant L_2-\phi \\ 0, & L_1-\phi \leqslant \Theta^1 \leqslant L_1, L_2 \leqslant \Theta^2 \leqslant L_2-\phi \end{cases}, \quad (108)$$

L_i being the length of graphene in the Θ^i-direction. Following Bedrossian and Kohn (2015), divide L_i, $i = 1, 2$ into l^{-1} regions of length l. On regions of area $\phi^2 l^2$ take the lower branch of Eq. (108), namely $u_3^f = 0$. On regions of area $(L_1 - \phi)l(L_2 - \phi)l$ we place a blister described by the above branch of Eq. (105). The area fraction $\phi = \frac{[(L_1-\phi)l,l]\times[(L_2-\phi)l,l]}{L_1L_2}$ is assumed to be a parameter (Bedrossian and Kohn, 2015). The bonded regions are that of area $\phi^2 l^2$ while the blistered regions are of area $(L_1 - \phi)l(L_2 - \phi)l$ (see Fig. 5 for a cross-section).

So, tension/compression that ultimately leads to delamination is described by the following expression for the graphene's displacement

$$u^f = \left(\epsilon\Theta^1, \Theta^2, \begin{pmatrix} \frac{L_1-\phi}{4\pi}\sin\left(\frac{4\pi\Theta^1}{L_1-\phi}\right)g(\Theta^2), & L_1 \leqslant \Theta^1 \leqslant L_1-\phi, L_2 \leqslant \Theta^2 \leqslant L_2-\phi \\ 0, & L_1-\phi \leqslant \Theta^1 \leqslant L_1, L_2 \leqslant \Theta^2 \leqslant L_2-\phi \end{pmatrix}\right). \quad (109)$$

Concurrently, we assume for the bulk material (the substrate) that displacement read

$$u^b = (\epsilon\Theta^1, \Theta^2, 0). \quad (110)$$

Thus, the substrate suffer no displacement out-of-surface. It perfectly bonds on areas $L_1 - \phi \leqslant \Theta^1 \leqslant L_1$, $L_2 \leqslant \Theta^2 \leqslant L_2 - \phi$, but it delaminates on areas $L_1 \leqslant \Theta^1 \leqslant L_1 - \phi$, $L_2 \leqslant \Theta^2 \leqslant L_2 - \phi$. We refer to the above branch of Eq. (109) as the delaminated part.

The outward unit normal for the film on the delaminated part read

$$\mathbf{n}^f = \left(-cos\left(\frac{4\pi\Theta^1}{L_1-\phi}\right)g(\Theta^2), -\epsilon\frac{L_1-\phi}{4\pi}\sin\left(\frac{4\pi\Theta^1}{L_1-\phi}\right)g'(\Theta^2), \epsilon\right). \quad (111)$$

By assuming that it has unit length, the curvature quantities related with the film render

$$b_{11}^f = u_{,11}^f \cdot \mathbf{n}^f = -\epsilon\frac{4\pi}{L_1-\phi}\sin\left(\frac{4\pi\Theta^1}{L_1-\phi}\right)g(\Theta^2), \quad (112)$$

$$b_{12}^f = u_{,12}^f \cdot \mathbf{n}^f = b_{21}^f = \epsilon\cos\left(\frac{4\pi\Theta^1}{L_1-\phi}\right)g'(\Theta^2), \quad (113)$$

$$b_{22}^f = u_{,22}^f \cdot \mathbf{n}^f = -\epsilon\frac{L_1-\phi}{4\pi}\sin\left(\frac{4\pi\Theta^1}{L_1-\phi}\right)g''(\Theta^2). \quad (114)$$

For the delaminated part, the first component of the shift vector read

$$p_1 = \frac{1}{c_9}[-\lambda(e_{11}^{0\,b} + e_{22}^{0\,b} + e_{33}^{0\,b})n_1^b - 2\mu e_{11}^{0\,b}n_1^b - 2\mu e_{12}^{0\,b}n_2^b - 2\mu e_{13}^{0\,b}n_3^b - \lambda\epsilon n_1^b - 2\mu\epsilon n_1^b - c_9p_1^0 + 2c_5e_{12}^{0\,f} + 2c_8b_{12}^{0\,f} - 2c_8b_{12}^f]. \quad (115)$$

For the second component of the shift vector we find

$$p_2 = \frac{1}{c_9}[-\lambda(e_{11}^{0\,b} + e_{22}^{0\,b} + e_{33}^{0\,b})n_2^b - 2\mu e_{21}^{0\,b}n_1^b - 2\mu e_{22}^{0\,b}n_2^b - 2\mu e_{23}^{0\,b}n_3^b - \lambda\epsilon n_2^b - c_9p_2^0 + c_5e_{11}^{0\,f} + c_5e_{22}^{0\,f} + c_8b_{11}^{0\,f} - c_8b_{22}^{0\,f} + c_5\epsilon + c_8b_{11} - c_8b_{22}]. \quad (116)$$

Then, the first of the momentum equation acquires the form

$$A(\Theta^1, \Theta^2)g''(\Theta^2) + B(\Theta^1, \Theta^2)g(\Theta^2) + \Gamma(\Theta^1, \Theta^2) = 0, \quad (117)$$

where

$$A(\Theta^1, \Theta^2) = 2\left(c_4 - \frac{c - 5c_8}{c_9}\right)\epsilon\sin\left(\frac{4\pi\Theta^1}{L_1-\phi}\right), \quad (118)$$

$$B(\Theta^1, \Theta^2) = -\left(c_3 - \frac{c_5c_8}{c_9}\right)\epsilon\frac{16\pi^2}{(L_1-\phi)^2}\sin\left(\frac{4\pi\Theta^1}{L_1-\phi}\right), \quad (119)$$

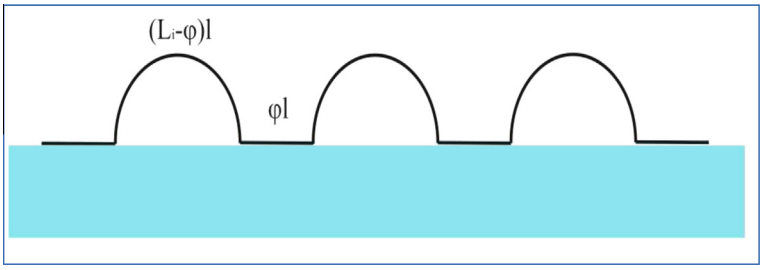

Fig. 5. A cross-section of the blister described by Eq. (108) in the i-direction.

$$\begin{aligned}\Gamma(\Theta^1,\Theta^2) &= \lambda(e_{11}^{0\,b}+e_{22}^{0\,b}+e_{33}^{0\,b})n_1^b+2\mu e_{11}^{0\,b}n_1^b+2\mu e_{12}^{0\,b}n_2^b\\ &+2\mu e_{13}^{0\,b}n_3^b+\lambda\epsilon n_1^b+2\mu\epsilon n_1^b+c_1e_{11,1}^{0\,f}+c_2e_{22,1}^{0\,f}+c_3b_{11,1}^{0\,f}\\ &+c_4b_{22,1}^{0\,f}-c_5p_{2,1}^0+\frac{c_1-c_2}{2}e_{12,2}^{0\,f}+\frac{c_3-c_4}{2}b_{12,2}^{0\,f}-2c_5p_{1,2}^0\\ &-\frac{c_5}{c_9}[-\lambda(e_{11}^{0\,b}+e_{22}^{0\,b}-e_{33}^{0\,b})n_2^b-2\mu e_{21}^{0\,b}n_1^b-2\mu e_{22}^{0\,b}n_2^b]_{,1}\\ &+\frac{c_5}{c_9}[-+2\mu e_{23}^{0\,b}n_3^b-\lambda\epsilon n_2^b-c_9p_2^0+c_5e_{11}^{0\,f}]_{,1}\\ &+\frac{c_5}{c_9}[c_5e_{22}^{0\,f}+c_8b_{11}^{0\,f}-c_8b_{22}^{0\,f}]_{,1}\\ &-2\frac{c_5}{c_9}[-\lambda(e_{11}^{0\,b}+e_{22}^{0\,b}-e_{33}^{0\,b})n_1^b-2\mu e_{11}^{0\,b}n_1^b-2\mu e_{12}^{0\,b}n_2^b]_{,2}\\ &+2\frac{c_5}{c_9}[-+2\mu e_{13}^{0\,b}n_3^b-\lambda\epsilon n_1^b-2\mu\epsilon n_1^b\\ &-c_9p_1^0+c_5e_{12}^{0\,f}+2c_8b_{12}^{0\,f}]_{,2}. \end{aligned}\tag{120}$$

Now consider the particular case where there exist a function $\Psi=\Psi(\Theta^1,\Theta^2)$ such that (Sfyris et al., 2008)

$$A(\Theta^1,\Theta^2)=\alpha\Psi(\Theta^1,\Theta^2),\tag{121}$$

$$B(\Theta^1,\Theta^2)=\beta\Psi(\Theta^1,\Theta^2),\tag{122}$$

$$C(\Theta^1,\Theta^2)=\gamma\Psi(\Theta^1,\Theta^2),\tag{123}$$

namely when

$$\frac{A(\Theta^1,\Theta^2)}{\alpha}=\frac{B(\Theta^1,\Theta^2)}{\beta}=\frac{C(\Theta^1,\Theta^2)}{\gamma}.\tag{124}$$

In this case the equation for the function f reads

$$\alpha g''(\Theta^2)+\beta g(\Theta^2)+\gamma=0.\tag{125}$$

We split Eq. (125) into a homogeneous and an inhomogenous part. We treat the homogenous part

$$\alpha g''(\Theta^2)+\beta g(\Theta^2)=0\tag{126}$$

using the technique of the characteristic polynomial. The characteristic polynomial has two roots: $\lambda_1=0,\ \lambda_2=-\frac{\beta}{\alpha}$, so we obtain the set of solutions

$$c_{11}e^{\lambda_1\Theta^2}+c_{22}e^{\lambda_2\Theta^2},\tag{127}$$

$c_{11},\ c_{22}$ being constants of integration. To these solutions we add the term $-\frac{\gamma}{\beta}$ which is a particular solution for Eq. (125). So, collectively for the function g satisfying Eq. (125) we find

$$g(\Theta^2)=c_{11}e^{\lambda_1\Theta^2}+c_{22}e^{\lambda_2\Theta^2}-\frac{\gamma}{\beta}.\tag{128}$$

The second branch of the delamination function render for the displacement of the film

$$u^f=(\epsilon\Theta^1,\Theta^2,0).\tag{129}$$

The displacement of the substrate is still described by Eq. (110). This is the part where the bonding is perfect. For this expression the function $g(\Theta^2)$ is identically zero. For the shift vector in this case we have

$$\begin{aligned}p_1 &= \frac{1}{c_9}[-\lambda(e_{11}^{0\ bulk}+e_{22}^{0\ bulk}+e_{33}^{0\ bulk})n_1-2\mu e_{11}^{0\ bulk}n_1\\ &-2\mu e_{12}^{0\ bulk}-2\mu e_{13}n_3-\lambda\epsilon n_1-2\mu\epsilon n_1-c_9p_1^0\\ &+2c_5e_{12}^{0\ film}],\end{aligned}\tag{130}$$

$$\begin{aligned}p_2 &= \frac{1}{c_9}[-\lambda(e_{11}^{0\ bulk}+e_{22}^{0\ bulk}+e_{33}^{0\ bulk})n_2-2\mu e_{21}^{0\ bulk}n_1\\ &-2\mu e_{22}^{0\ bulk}-2\mu e_{23}n_3-\lambda\epsilon n_2-c_9p_2^0+c_5e_{11}^{0\ film}\\ &+c_5e_{22}^{0\ film}+c_5\epsilon].\end{aligned}\tag{131}$$

Substituting this to the momentum equation render conditions that should be satisfied in order the delamination function Eq. (109) to be a solution.

To sum up, we treat the delamination by differentiating between $\mathbf{u}^f$ and $\mathbf{u}^b$. While $\mathbf{u}^b$ is given by Eq. (110), film's displacement has two branches. The first branch of Eq. (109) describe areas where delamination take place; essentially, there $\mathbf{u}^f\neq\mathbf{u}^b$. On the second branch of Eq. (109) there is perfect bonding, thus $\mathbf{u}^f=\mathbf{u}^b$. Eqs. (109) and (110) qualify as solutions for the problem at hand, provided in delamination areas, $L_1-\phi\leqslant\Theta^1\leqslant L_1,\ L_2-\phi\leqslant\Theta^2\leqslant L_2$, the shift components are given by Eqs. (115) and (116), the function g is given by Eq. (128) and also Eqs. (124) are satisfied. In areas of perfect bonding the shift components are given by Eqs. (130) and (131) and the function g is zero. To all these conditions one should add the second equation of momentum and the moment of momentum equation which can be obtained straightforwardly.

6. Conclusions

We drawn motivation from Androulidakis et al. (2014) where we study the axial compression of a graphene monolayer on a polymeric substrate, using Raman spectroscopy. In our work here, we study theoretically, and model mathematically using continuum mechanics, that experimental setup expanding on previous works that included the graphene only. More specifically, we split our analysis in two major areas: firstly, the case when the graphene and the substrate are perfectly bonded, and secondly the case when partial delamination appears between them.

The perfect bonding can be further categorized to in-surface motions only and out-of-surface motions. If out-of-surface motion of graphene is prohibited, we study biaxial tension/compression and simple shear. When out-of-surface motion of graphene is allowed, we face a much more difficult problem and find specific solution under certain conditions. Partial delamination of the graphene from the polymeric substrate is an undesirable phenomenon that appears frequently in the manufacturing, treatment and testing of graphene monolayers. In our analysis, we study a specific

Please cite this article in press as: Sfyris, D., et al. Graphene resting on substrate: Closed form solutions for the perfect bonding and the delamination case. Int. J. Solids Struct. (2015), http://dx.doi.org/10.1016/j.ijsolstr.2015.06.024

form of delamination in the form of a blister. We report conditions for such a blister to be a solution of the problem.

Acknowledgments

We sincerely thank both reviewers for most valuable comments and especially for bringing to our attention a mistake in the first version of the draft. We thank G.I. Sfyris (Athens, Greece) for reading the manuscript throughout and making most valuable additions. This research has been co-financed by the European Union (European Social Fund ESF) and Greek national funds through the Operational Program Education and Lifelong Learning of the National Strategic Reference Framework (NSRF) Research Funding Program: ERC-10 Deformation, Yield and Failure of Graphene and Graphene-based Nanocomposites. The financial support of the European Research Council through the projects ERC AdG 2013 (Tailor Graphene) is gratefully acknowledged.

Appendix A. Supplementary data

Supplementary data associated with this article can be found, in the online version, at http://dx.doi.org/10.1016/j.ijsolstr.2015.06.024.

References

Androulidakis, C., Koukaras, E.N., Frank, O., Tsoukleri, G., Sfyris, D., Parthenios, J., Pugno, N., Papagelis, K., Novoselov, K.S., Galiotis, C., 2014. Failure processes in embedded monolayer graphene under axial compression. Sci. Rep. 4, 5271.

Bedrossian, J., Kohn, R.V., 2015. Blister patterns and energy minimization in compressed thin films on compliant substrates. Commun. Pure Appl. Math. 68, 472–510.

Cadelano, E., Palla, P.L., Giordano, S., Colombo, L., 2009. Nonlinear elasticity of monolayer graphene. Phys. Rev. Lett. 102, 235502.

Cao, Y., Hutchinson, J.W., 2012. Wrinkling phenomena in neo-Hookean film/substrate systems. J. Appl. Mech. 79 (031010), 1–9.

Chhapadia, P., Mohammadi, P., Sharma, P., 2011. Curvature-dependent surface energy and implications for nanostructures. J. Mech. Phys. Sol. 59, 2103–2115.

Ericksen, J.L., 1970. Nonlinear elasticity of diatomic crystals. Int. J. Sol. Struct. 6, 951–957.

Ericksen, J.L., 1979. On the symmetry of deformable crystals. Arch. Ration. Mech. Anal. 72, 1–13.

Fadda, G., Zanzotto, G., 2000. The arithmetic symmetry of monoatomic 2-nets. Acta Crystallogr. A 56, 36–48.

Fadda, G., Zanzotto, G., 2001. Symmetry breaking in monoatomic 2-lattices. Int. J. Non-Linear Mech. 36, 527–547.

Fried, E., Todres, R.E., 2005. Mind the gap: the shape of the free surface of a rubber-like material in proximity to a rigid contactor. J. Elast. 80, 97–151.

Galiotis, C., Frank, O., Koukaras, E.N., Sfyris, D., in press. Graphene mechanics: current status and perspectives. Annu. Rev. Chem. Biomol. Eng. http://dx.doi.org/10.1146/annurev-chembioeng-061114-123216.

Huang, R., 2005. Kinetic wrinkling of an elastic film on a viscoelastic substrate. J. Mech. Phys. Sol. 53, 63–89.

Lee, C., Wei, X.D., Kysar, J.W., Hone, J., 2008. Measurement of the elastic properties and instrinsic sternght of monolayer graphene. Science 321, 385–388.

Mishnaevsky, L.L., Gross, D., 2005. Deformation and failure in thin films/substrate systems: methods of theoretical analysis. ASME Appl. Mech. Rev. 58, 338–353.

Murnaghan, F.N., 1951. Finite Deformation of an Elastic Solid. John Wiley.

Parry, G., 1978. On diatomic crystals. Int. J. Sol. Struct. 14, 281–287.

Pitteri, M., 1984. Reconciliation of local and global symmetries of crystals. J. Elast. 14, 175–190.

Pitteri, M., 1985. On $\nu + 1$ lattices. J. Elast. 15, 3–25.

Pitteri, M., Zanzotto, G., 2003. Continuum Models for Phase Transition and Twinning in Crystals. Chapman and Hall, Boca Raton.

Puntel, E., Deseri, L., Fried, E., 2011. Wrinkling of a stretched thin sheet. J. Elast. 105, 137–170.

Rivlin, R., 1963. The solution of problems in second order elasticity. J. Ration. Mech. Anal. 2, 53–81.

Sfyris, D., Galiotis, C., in press. Curvature dependent surface energy for free standing monolayer graphene. Math. Mech. Sol. http://dx.doi.org/10.1177/1081286514536367.

Sfyris, D., Charalambakis, N., Kalpakides, V.K., 2008. Continuously dislocated bodies with a neo-Hookean like energy subjected to antiplane shear. J. Elast. 93, 245–262.

Sfyris, D., Sfyris, G.I., Galiotis, C., 2014a. Curvature dependent surface energy for free standing monolayer graphene. Some closed form solutions of the nonlinear theory. Int. J. Nonlinear Mech. 67, 186–197.

Sfyris, D., Sfyris, G.I., Galiotis, C., 2014b. Curvature dependent surface energy for free standing monolayer graphene. Geometrical and material linearization with closed form solutions. Int. J. Eng. Sci. 85, 224–233.

Sfyris, D., Sfyris, G.I., Galiotis, C., in press. Constitutive modeling of some 2D crystals: graphene, hexagonal BN, MoS_2, WSe_2 and $NbSe_2$. Int. J. Sol. Struct. http://dx.doi.org/10.1016/j.ijsolstr.2015.03.030.

Sfyris, D., Koukaras, E.N., Pugno, N., Galiotis, C., submitted for publication. Graphene as a hexagonal 2-lattice: evaluation of the in-plane material constants for the linear theory. A multiscale approach.

Steigmann, D.J., Ogden, R.W., 1999. Elastic surface-substrate interactions. Proc. R. Soc. Lond. A 455, 437–474.

Wang, Z.Q., Zhao, Y.P., Huang, Z.P., 2010. The effects of surface tension on the elastic properties of nano structures. Int. J. Eng. Sci. 48, 140–150.

Wei, X., Fragneand, B., Marianetti, C.A., Kysar, J.W., 2009. Nonlinear elastic behavior of graphene: ab initio calculations to continuum description. Phys. Rev. B 80, 205407.

<www.mit.edu/6.777/matprops>.